Synthesis and functions of coordination materials which show unique structural changes responding to external stimuli

静岡大学博士論文

Synthesis and Functions of Coordination Materials which Show Unique Structural Changes Responding to External Stimuli

（外部刺激に応答して構造を変化させる配位化合物の合成と機能）

平成２１年６月

大学院理工学研究科

物質科学専攻

宮澤　誠

Acknowledgements

This work has been carried out at Graduate School of Chemistry, Faculty of Science, Shizuoka University under the direction of Associate Professor Mitsuru Kondo. The author wishes to thank to his helpful guidance and discussion. The author also acknowledges Professor Hiroyuki Kawaguchi of Tokyo Institute Technology for the measurements of single crystal X-ray analysis. The author would like to thank to Professor Hisao Murai for his helpful discussion and guidance of this work. The author wishes to thank to Mr. R. Ikeya in Center for Instrumental Analysis for his contribution for single crystal X-ray analysis. The author wishes to thank to Mr. Yasuhiko Irie, Mr. Takahiro Iwase, Miss Yuri Hayakawa for their collaborations of the research. The author also wishes to thank to all member of Kondo research group for their encouragement. The author would like to thank to the Iketani Science Foundation for the support in research fund.

Contents

Chapter 1

General Introduction

Coordination polymer has shown unique functions such as molecular adsorption, heterogeneous catalysis, molecular magnetism, non-linear optics, and so on. Since these functions are largely dependent on the network structures, synthesis of new network structures has attracted intense attention. Among numerous coordination polymers have developed to date, dynamic coordination polymers that change their structures responding to external stimuli are expected to give novel functions, such synthetic studies were not well explored.

One of the target networks structure is the creation of porous networks, which reversibly change the channel structures responding to the external stimuli such as physical stimuli, and solvents. I have succeeded in creation of new coordination polymers whose structures are reversibly interconverted between two structures. For example, $[Zn_2(oba)_4(dmf)_2]$ (oba = 4,4'-oxybis(benzoate)) (**1**) switches to $[Zn(oba)_2(H_2O)_2]$ (**2**) by contact with water, and the former is reproduced by immersing of the latter in DMF. Complex **1** has nano-scale channels, while Complex **2** shows a non-porous structure. That is, this system is a unique dynamic coordination network system. (Chapter 2 and 3)

On the other hand, $[Ni(ima)_2(MeOH)_2]$ (ima = 4-imidazoleacetate) (**3**) shows a unique network structure with large one-dimensional channels. The channels contain no guest molecules, and maintain useful for inclusions of guest molecules. Complex **3** loses their MeOH molecules on heating at 100°C under reduced pressure to give $[Ni(ima)_2]$ (**3b**), which is an

amorphous material. Complex **3b** changes to **3** by contact with MeOH, accompanying recreation of channel structures. Interestingly, this process is induced by MeOH molecule selectively. I have clarified the unique structural recovers, and found that the recovers induce the adsorption of other guest molecules. That is, adsotpions of EtOH molecules by contact with MeOH molecules are observed. This unique switching process is novel in that the inclusions of larger EtOH molecule is included by contact with MeOH. (Chapter 4)

In addition to the dynamic coordination frameworks, which change their structures responding to organic solvents, I have explored a novel dynamic coordination polymer which changes their channel structures responding to temperature variation. Complex $[Ni(dps)_2(NO_3)_2]EtOH$ (dps = 4,4'-dipyridylsulfide) (**4**) reveals the phase transition depending on the temperature variation. The structural changes diminish at low temperature, and recovers at room temperature. Particularly, mechanical encapsulations of ethanol molecules at the closed channel created at low temperature are observed. This unique reversible structural change of channels is unprecedented, and novel in the porous materials. (Chapter 5)

These unique dynamic coordination polymers are constructed by flexible ligands. That is, these ligands contain flexible sites such as ether, sulfide, and methylene groups. I have focused on the studies of the coordination polymers obtained by flexible bridging ligands. Although redox property is attractive functions of polymer materials, syntheses of coordination polymers with redox properties are still limited. In the background, I have selected two bridging ligands redox-active bridging ligands, i.e. 4,4'-sulfonyldibenzoate (dbsf), 5,5'-thiodisalicylate (tdsa), 4,4'-sulfonyldiphenolate (sdp), and cobaltoceneium(III)dicarboxylate (ccdc) to develop new dynamic coordination polymers. Among the ligands, tpyta gives a 1-dimensional chiral

helices. Interestingly, only one helical orientation is involved in the crystal structure, exhibiting a spontaneous resolution from achiral materials. This complex demonstrates the high redox properties ascribed to the sulfide sites. (Syntheses and characterizations of similar redox active coordination polymers were obtained from bridging ligands, dbsf, tdsa, sdp. (Chapter 6) These complexes were clarified by single crystal X-ray analyses and electrochemistry.

Metallocene is one of the typical redox active and flexbile units. I have synthesized a new high redox active coordination polymer $[Cu(ccdc)_2]$ (**5**), which was a first example of coordination network, which include cobaltocene units. This complex shows a 2-dimensional framework, which create cage between the layers, which trap the MeOH molecules within it. This complex reveals high redox property depending on the ccdc unit. (Chapter 7)

Chapter 2.

Dynamic Coordination Polymers with 4,4'-Oxybis(benzoate). Reversible Transformations of Nano- and Non-porous Coordination Frameworks Responding to Guest Molecules

Abstract

Reversible construction of a nano-porous framework from a non-porous framework has been found in the zinc(II) coordination polymer with 4,4'-oxybis(benzoate) (oba). $[Zn_2(oba)_2(dmf)_2]$, which has 1 nm scale channels, transforms to the non-porous coordination polymer $[Zn(oba)(H_2O)]$ with the loss of porosity. The obtained compound reversibly yields the starting nano-porous framework upon treatment with DMF.

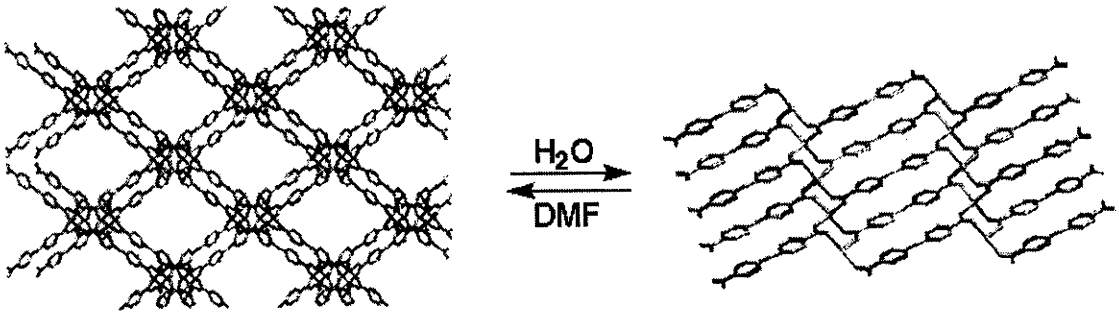

Introduction

Coordination polymers with porous frameworks have attracted attention as a new class of porous materials because these materials have shown new porous functions that are not found in inorganic porous materials such as zeolites and graphite.[1-7] For example, heterogeneous catalysis,[2] anion exchange,[3] molecular adsorption and storage[4] have been reported to date. Their frameworks are flexible in many cases, and various new dynamic porous frameworks have been created.[5-7] One of the recent interests in this field is the reversible transformation between a nano-porous framework and a non-porous framework accompanying the enforced release and readsorption of guest molecules. For example, recently, Pan et al.[6] have reported a recyclable nano-porous coordination framework that changes to a non-porous framework by addition of water with loss of a pillar framework ligand, 4,4'-bipyridine (4,4'-bpy). This reaction enforces the release of the included guest molecules. Moreover, treatment of the resulting non-porous framework with 4,4'-bpy in dmf at 150 °C reproduces the original porous framework.

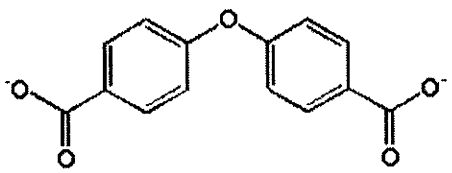

oba

Scheme 1

We have focused on the synthesis of new coordination networks with chalcogen atoms in the organic backbone.[8] Recently, we selected 4,4'-oxybis(benzoate) (oba; Scheme 1) as a

bridging ligand for creation of new coordination frameworks, and have succeeded in the synthesis of the two new nano-porous coordination polymers, $[Zn_2(oba)_2(dmf)_2]\cdot 2dmf$ (**1**) and $[Zn(oba)(H_2O)]$ (**2**), a new nano-porous coordination polymer and a non-porous polymer, respectively. Here, we report the synthesis, structures, and the unique dynamic structural changes that reversibly transform their frameworks, depending on the accessible solvents, with loss and recreation of the porosity.

Result and discussion

The new nano-porous coordination polymer **1** was obtained as highly moisture-sensitive colorless crystals by the reaction of $Zn(CH_3COO)_2\cdot 2H_2O$ with H_2oba in dry dmf. The structure of **1** was characterized by single crystal X-ray analysis.[9] As shown in Figure 1, **1** has a two-dimensional framework, which is constructed by connections of dinuclear zinc units with oba ligands. Although the network motif is similar to those of $[Cu_2(1,4\text{-benzenedicarboxylate})_2]$[4b] and $[Zn_2(1,4\text{-benzenedicarboxylate})_2(dmf)_2]$,[4d] the bent oba structure provides a new unique structural aspect in the channel shape and thickness of the layer. That is, the oba ligand is largely bent at the ether-oxygen sites (C–O–C = 121.8(4)°), causing an undulation along the *c*-axis. As a result, the cavity shape deviates from a regular square to a rhombus with size of about 17 Å × 11 Å along the two diagonal directions. The bent structure of oba also contributes about 11 Å of the thickness of the layer, in which ether-oxygen sites of oba remarkably stick out from the plane. In spite of the large cavities, these layers stack along the *b*-axis without interpenetration. The thickness of the layer could inhibit the possibility of interpenetration.

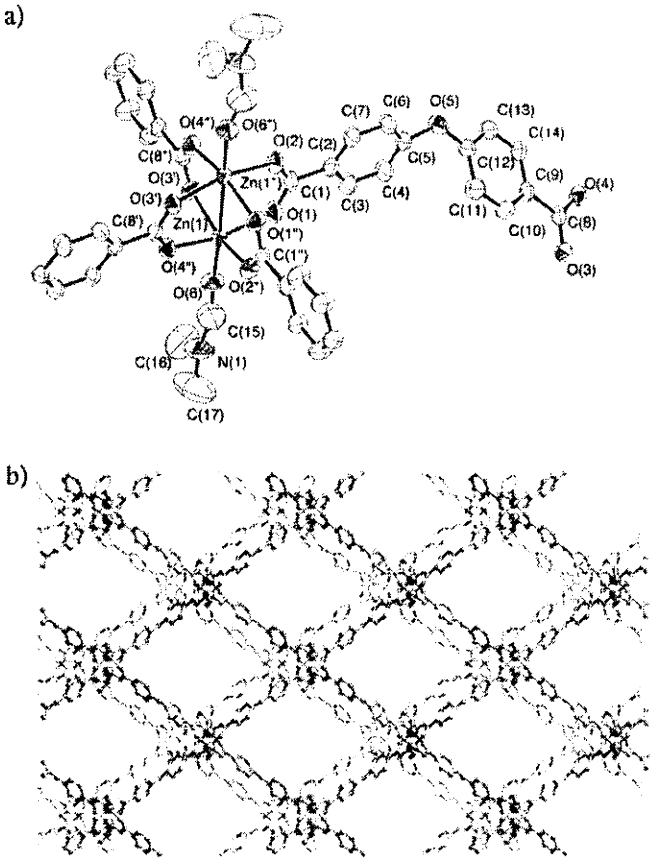

Figure 1. Structure of **1**. ORTEP view around the dizinc center (a) and the stacked aspect of the two-dimensional layers (b), in which alternate layers are shown by red and blue colors, respectively.

As shown in Figure 1b, **1** creates nano-scale channels along the *b*-axis. The channel size is about 13 Å × 9 Å, which is slightly contracted compared with the cavity size of each layer because of the slight alternate slides of the stacked layers (these two layers are illustrated as blue and red frameworks in Figure 1b). The channels are filled with two free dmf molecules per one dinuclear unit. We monitored the changes of the X-ray powder diffraction (XRPD) patterns of **1** under air to study the stability or dynamic property of the moisture-sensitive framework. This experiment demonstrated that **1** transforms to a new

crystalline material via an amorphous state because of reaction with H_2O (a similar change was also induced by immersing **1** in water).

For the structural characterization of the product obtained from **1** and water, we prepared a new coordination polymer **2** from the aqueous reaction mixture of $Zn(NO_3)_2 \cdot 6H_2O$ and H_2oba in the presence of base. We confirmed that **2** is a reaction product of **1** with H_2O by comparing the simulated XRPD pattern based on the atomic coordinates of **2** and the observed pattern of the obtained product.

The structure of **2** is shown in Figure 2,[10] in which the framework arrangement is similar to that of the previously reported $[Cd(oba)_2(H_2O)]$.[11] Each Zn center forms a distorted trigonal bipyramid with four carboxylate oxygen atoms from oba and one water molecule. The two carboxylate moieties of the oba bridge each Zn center to produce one-dimensional $(Zn\text{-}oba)_n$ chains. These chains are further connected by the oba-frameworks to yield a two-dimensional structure. Similar to **1**, these layers are not planar but undulated due to the bending at the ether-oxygen sites of the oba ligand. The coordinating waters between the layers form hydrogen bonds with the two carboxylate-oxygen atoms of the oba in the adjacent layer. As a result, a three-dimensional network is constructed. Because the water molecules are tightly included between the layers by the coordination and hydrogen bonds, these are not released below 190 °C, as demonstrated by thermogravimetric analysis.

In spite of the different framework structures, as mentioned above, **1** readily transforms to **2** by addition of water. Furthermore, we found that the reverse transformation—i.e., formation of **1** from **2**—also proceeds under mild conditions—i.e., by

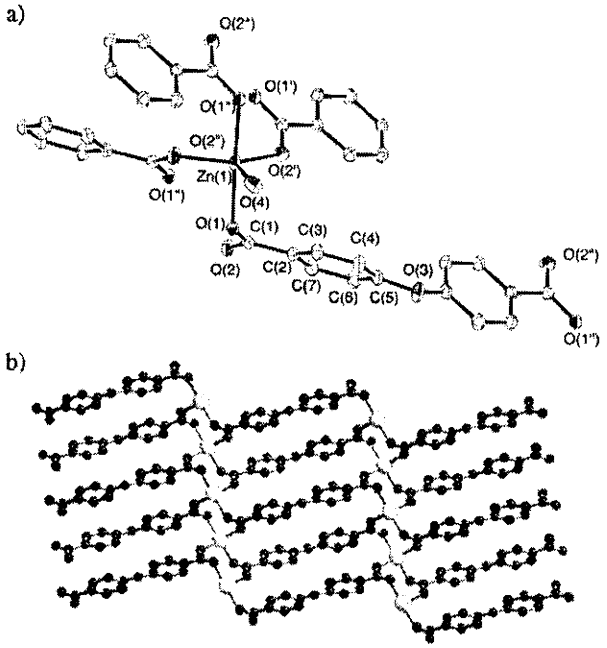

Figure 2. Structure of **2**. ORTEP view around the zinc center (a) and the two-dimensional network (b).

addition of dmf to **2** and standing for three days. These structural changes were monitored by the changes in the XRPD peaks, which are summarized in Figure 3. The XRPD peaks for **1** (Figure 3a) disappear within 20 minutes under air due to the change to an amorphous state (Figures 3b). After one day, the resulting powder shows a new XRPD pattern due to the formation of **2** (Figures 3c). Some drops of dmf solvent on the resulting powder reproduce XRPD peaks for **1** after three days (Figures 3d). Although crystal shape and size seem to be retained during the transformation between **1** and **2**, these processes are not single-crystal-to-single-crystal,[7] but proceed via an amorphous state. Neither structural

transformation is induced by other general organic guests, such as benzene, dioxane, alcohols, THF, and acetonitrile within a few weeks, demonstrating that these structural reconstitutions would proceed with high guest selectivity.

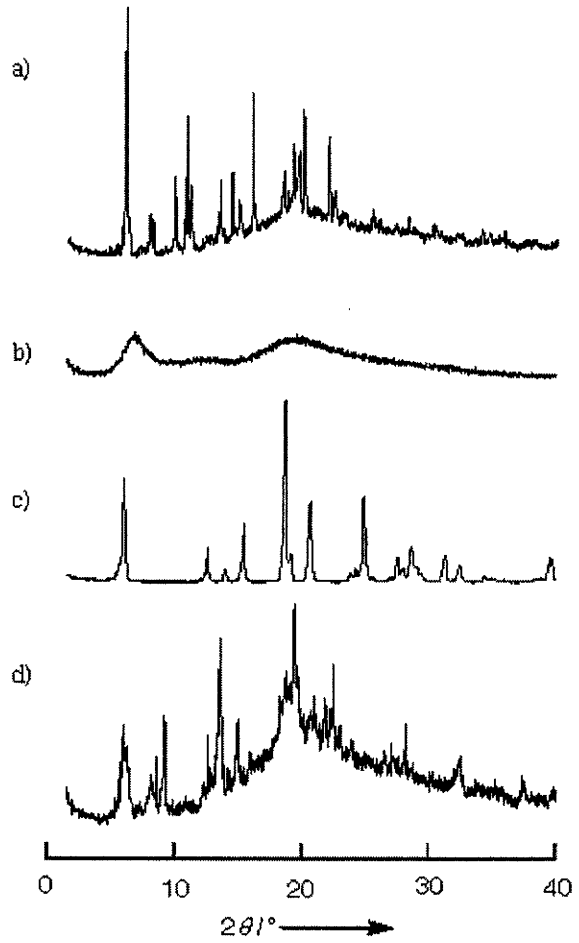

Figure 3. XRPD pattern of a fresh sample of **1** (a), which changes to amorphous under air (b), followed by **2** (c). The original pattern for **1** was regained (d) after the addition of a few drops of dmf to **2**.

Although a similar transformation has been reported by Pan et al.,[6] that system accompanies the loss of 4,4'-bpy upon formation of the non-porous framework, therefore addition of 4,4'-bpy is necessary for recreation of the nano-porous framework under vigorous

reaction conditions (150 °C in dmf for three days). In contrast, our system is superior in that the transformation proceeds under mild conditions without the addition or loss of the bridging ligands. Moreover, to the best of our knowledge, this is the first example that a nano-porous framework having channels larger than 10 Å is reversibly created from a non-porous framework. Further studies of the functions based on this dynamic framework are in progress.

Experimental

1: A DMF solution (200 mL) of 4,4'-H_2oba (5.2 g, 20 mmol) was allowed to diffuse into a DMF solution (200 mL) of $Zn(CH_3COO)_2 2H_2O$ (2.2 g, 10 mmol). The colorless cubic crystals formed within 3 days were collected by filtration under N_2 atmosphere. Elemental analysis (%)

2: An aqueous solution (100 mL) of 4,4'- H_2oba (1.29 g, 5 mmol) was allowed to diffuse into an aqueous solution of $Zn(NO_3)_2 6H_2O$ (1.49 g, 5.0 mmol) and excess NEt_3. The colorless crystals obtained after 1 week were collected by filtration.

References

[1] a) S. Subramanian, M. J. Zawototko, *Angew. Chem. Int. Ed.* **1995**, *34*. 2127; b) M. J. Zaworotko, *Angew. Chem. Int. Ed.* **1998**, *37*, 1211; c) G. Kepert, J., M. J. Rosseinsky, *Chem. Commun.* **1999**, 375; d) P. J. Hagrman, D. Hagrman, J. Zubieta, *Angew. Chem. Int. Ed.* **1999**, *38*, 2638; e) O. M. Yaghi, G. Li, H. Li, *Nature* **1995**, *378*, 703; f) O. M. Yaghi, H. Li, C. Davis, D. Richardson, T. L. Groy, *Acc. Chem. Res.* **1998**, *31*, 474;

g) S. Kitagawa, M. Kondo, *Bull. Chem. Soc. Jpn.* **1998**, *71*, 1739; h) C. Janiak, *J. Chem. Soc., Dalton Trans.* **2003**, 2781.

[2] for example, a) M. Fujita, Y. J. Kwon, S. Washizu, K. Ogura, *J. Am. Chem. Soc.* **1994**, *116*, 1151; b) J. S. Seo, D. Whang, H. Lee, S. I. Jun, J. Oh, Y. J. Jeon, K. Kim, *Nature* **2000**, *404*, 982.

[3] for example a) B. F. Hoskins, R. Robson, *J. Am. Chem. Soc.* **1990**, *112*, 1546; b) O. M. Yaghi, H. Li, *J. Am. Chem. Soc.* **1995**, *117*, 10401; c) O. M. Yaghi, H. Li, *J. Am. Chem. Soc.* **1996**, *118*, 295.

[4] for example a) M. Kondo, T. Yoshitomi, K. Seki, H. Matsuzaka, S. Kitagawa, *Angew. Chem. Int. Ed.* **1997**, *36*, 1725; b) W. Mori, K. Inoue, H. Yoshida, S. Nakayama, S. Takamizawa, M. Kishita, *Chem. Lett.* **1997**, 1219; c) H. Li, M. Eddaoudi, T. L. Groy, O. M. Yaghi, *J. Am, Chem. Soc.*, **1998**, *120*, 8571. d) H. Li, M. Eddaoudi, M. O'Keeffe, O. M. Yaghi, *Nature* **1999**, *402*, 276; e) H. J. Choi, T. S. Lee, M. P. Suh, *Angew. Chem. Int. Ed.* **1999**, *38*, 1405; f) K. Seki, *Chem. Commun.* **2001**, 1496.

[5] a) K. Kasai, M. Aoyagi, M. Fujita, *J. Am. Chem. Soc.* **2000**, *122*, 2140; b) D. Li, K. Kaneko, *Chem. Phys. Lett.* **2001**, *335*, 50. c) R. Kitaura, K. Fujimoto, S. Noro, M. Kondo, S. Kitagawa, *Angew. Chem. Int. Ed.* **2002**, *41*, 133.

[6] L. Pan, H. Liu, X. Lei, X. Huang, D. H. Olson, N. J. Turro, J. Li, *Angew. Chem.* **2003**, *115*, 560.

[7] a) K. Biradha, M. Fujita, *Angew. Chem. Int. Ed.* **2002**, *41*, 3392; b) M. P. Suh, J. W. Ko, H. J. Choi, *J. Am. Chem. Soc.* **2002**, *124*, 10976; c) S. Takamizawa, E.-i. Nakata, H. Yokoyama, K. Mochizuki, W. Mori, *Angew. Chem. Int. Ed.* **2003**, *115*, 4467.

[8] M. Kondo, M. Miyazawa, Y. Irie, R. Shinagawa, T. Horiba, A. Nakamura, T. Naito, K. Maeda, S. Utsuno, F. Uchida, *Chem. Commun.* **2002**, 2156.

[9] X-ray crystallographic data for **1**: $C_{40}H_{44}N_4O_{14}Zn_2$, M_r = 935.57, orthorhombic, space group *P*nna (no. 52), a = 23.79(1), b = 15.887(7), c = 17.773(8) Å, V = 6716(4) Å^3, Z = 4, m(MoKa) = 0.759 mm^{-1}, T = 293 K, R = 0.059, wR = 0.063 for 2951 unique reflections (R_{int} = 0.061) with $I > 2s(I)$ and 246 parameters.

[10] X-ray crystallographic data for **2**: $C_{14}H_{10}O_6Zn$, M_r = 339.61, monoclinic, space group $P2_1$ (no. 13), a = 7.391(6), b = 6.273(5), c = 14.256(11) Å, b = 103.572(10)°, V = 642.5(8) Å^3, Z = 2, m(MoKa) = 1.937 mm^{-1}, T = 293 K, R = 0.057, wR = 0.065 for 1660 unique reflections (R_{int} = 0.028) with $I > 2s(I)$ and 101parameters.

[11] M. L. Hu, P. Gao, S. W. Ng, *Acta Cryst.* **2002**, *C58*, m323.

[12] A. Altomare, G. Cascarano, C. Giacovazzo and A. Guagliardi; *J. Appl. Crystallogr.*, **1993**, *26*, 343.

Chapter 3.

Synthesis and Structural Determination of New Multidimensional Coordination Polymers with 4,4'-Oxybis(benzoate) Building Ligands: Construction of Coordination Polymers with Heteroorganic Bridges

Abstract

We report on the synthesis and crystal structures of three new zinc coordination polymers with 4,4'-oxybis(benzoate) (oba) ligands. Single crystals of $[Zn_2(oba)_2(azpy)(dmf)_2]\cdot 6DMF$ (azpy = 4,4'-azopyridine) and $[Zn_2(oba)_2(bpe)]\cdot 2DMF\cdot 4H_2O$ (bpe = trans-1,2-bis(4-pyridyl)ethylene) were prepared by treatment of $Zn(CH_3COO)_2\cdot 2H_2O$ with the H_2oba and bis-pyridine type ligands, azpy and bpe, respectively, in DMF. Compound $[Zn_2(oba)_2(azpy)(dmf)_2]\cdot 6DMF$ has a unique ladder structure comprising of heteroorganic bridges, in which the Zn-oba chains construct the side rails, while the Zn–azpy–Zn parts construct the rungs of the ladder framework. Despite the large size of the cavities, these ladder chains stack without interpenetration, and the cavities in the ladder framework are partially connected to create one-dimensional channel-like cavities. Compound $[Zn_2(oba)_2(bpe)]\cdot 2DMF\cdot 4H_2O$ exhibits a three-dimensional coordination framework that is comprised of heteroorganic bridges. The framework is interwoven by two-dimensional layers of

$[Zn_2(oba)_2]$ and the Zn_2-bpe chains. The three-dimensional framework, which contains large cavities, about 13 × 11 $Å^2$ in area, has a high porosity and a density of only 0.53 gcm^{-3}.

Introduction

The construction of coordination polymers with new network motifs is of current interest for the development of new functional materials and in fundamental studies of crystal engineering and supramolecular chemistry [1-8]. In the synthesis of new network structures, coordination polymers constructed from heteroorganic bridges are challenging subjects because any synthetic method used needs to take into account the designed construction involving versatile coordination frameworks [9-12]. Nevertheless, coordination networks constructed from heteroorganic bridges are rare because of the difficulty in achieving the rational incorporation of different organic ligands.

Bis-benzoate-type bridges have been exploited in the synthesis of many coordination networks [7, 13-16]. For example, $[M_2(1,4\text{-benzenedicarboxylate})_2]$-type frameworks have been prepared and characterized [17]. The unique feature of this type of network structure is the presence of square cavities, which are retained without collapsing and exhibit porous functionalities such as gas adsorption and heterogeneous catalysts. Although it has been shown that the two-dimensional layers can be connected by additional neutral ligands, structural characterization from X-ray single crystal analysis has not been carried out.

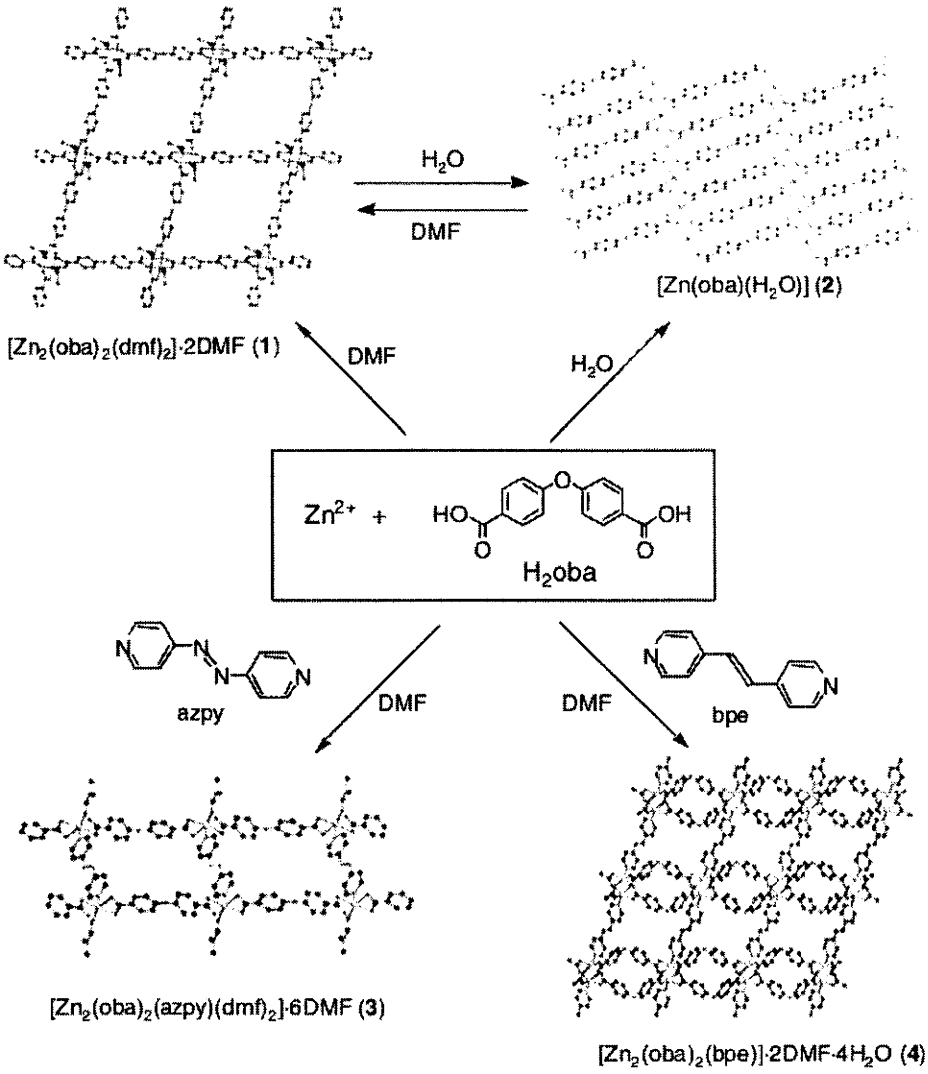

Figure 1. The summary of Zn—oba network system found in this work

We have investigated coordination polymers with chalcogen atoms in the organic bridging ligands [18-20], and have reported on two coordination polymers, $[Zn_2(oba)_2(dmf)_2]\cdot 2DMF$ (oba = 4,4'-oxybis(benzoate)) (**1**) and $[Zn(oba)(H_2O)]$ (**2**) in a recent communication. These two compounds show reversible structural transformations depending on the present solvents. In ongoing work, we have successfully created two new zinc coordination polymers constructed from heteroorganic bridges: oba- and bis-pyridine-type ligands, i.e.,

trans-1,2-bis(4-pyridyl)ethylene (bpe) and 4,4'-azopyridine (azpy). Despite the similar structures of the two ancillary ligands, the structures of the resulting compounds, $[Zn_2(oba)_2(azpy)(dmf)_2]\cdot 6DMF$ (azpy = 4,4'-azopyridine) (**3**) and $[Zn_2(oba)_2(bpe)]\cdot 2DMF\cdot 4H_2O$ (**4**), show different network structures. The network motifs of these compounds are illustrated in Figure 1. This paper describes the synthesis and crystal structures of coordination polymers **3** and **4**.

Result and discussion

Diffusion of a DMF solution of H_2oba and azpy into a DMF solution of $Zn(CH_3COO)_2\cdot 2H_2O$ yielded single crystals of Compound **3**. An ORTEP view around the zinc centers is shown in Figure 2a. The selected bond distances and angles are listed in Table 1. The carboxylate ligands of the oba group bind to the zinc center via a four-membered chelation, in which the two Zn–O bond distances differ significantly: Zn(1)–O(1) = 2.091(3) Å, Zn(1)–O(2) = 2.231(3) Å, Zn(1)–O(3) = 2.283(4) Å, and Zn(1)–O(4) = 2.096(3) Å. In addition to the four carboxylate oxygen atoms, an additional oxygen atom of a dmf molecule and a pyridine nitrogen atom of an azpy group are coordinated to the zinc center. The above coordination center is based on the markedly distorted octahedron observed. This is due to the four-membered carboxylate chelation, in which the N(1) atom of the azpy group and the O(3) atom of the oba group occupy the axial positions at the N(1)–Zn(1)–O(3) group with a bond angle of 151.2(1)°.

Table 1. Selected bond distances (Å) and angles (°) for Compound **3**.

Zn(1)—O(1)	2.091(3)	Zn(1)—O(2)	2.231(3)
Zn(1)—O(3*)	2.283(4)	Zn(1)—O(4*)	2.096(3)
Zn(1)—O(6)	2.042(3)		
O(1)—Zn(1)—O(2)	60.5(1)	O(1)—Zn(1)—O(3*)	105.5(1)
O(1)—Zn(1)—O(4*)	156.4(1)	O(1)—Zn(1)—O(6)	95.3(1)
O(1)—Zn(1)—N(1)	102.6(1)	O(2)—Zn(1)—O(3*)	92.3(1)
O(2)—Zn(1)—O(4*)	99.7(1)	O(2)—Zn(1)—O(6)	155.5(1)
O(2)—Zn(1)—N(1)	96.0(1)	O(3*)—Zn(1)—O(4*)	59.6(1)
O(3*)—Zn(1)—O(6*)	90.6(1)	O(3*)—Zn(1)—N(1)	151.2(1)
O(4*)—Zn(1)—O(6)	102.7(1)	O(4*)—Zn(1)—N(1)	91.7(1)
O(6)—Zn(1) —N(1)	93.2(1)		

symmetry equivalent positions; * = x, y, z

Each zinc center is bridged by an oba group to yield a one-dimensional chain directed along the *b*-axis. The chains are further connected by azpy bridges to yield a ladder-type one-dimensional structure, as shown in Figure 2b, in which the Zn-oba chains construct the "side rails", and the Zn–azpy–Zn parts construct the "rungs" of the ladder framework. The Zn···Zn distances bridged by the oba and azpy groups are 14.1 Å and 13.1 Å, respectively, which form large cavities with an effective area of about 12 × 11 $Å^2$. The cavities in the framework exhibit a compressed octahedral structure at the apexes of the four zinc atoms and two ether-oxygen atoms. The coordinating dmf molecules protrude in the same direction as the corresponding side rail.

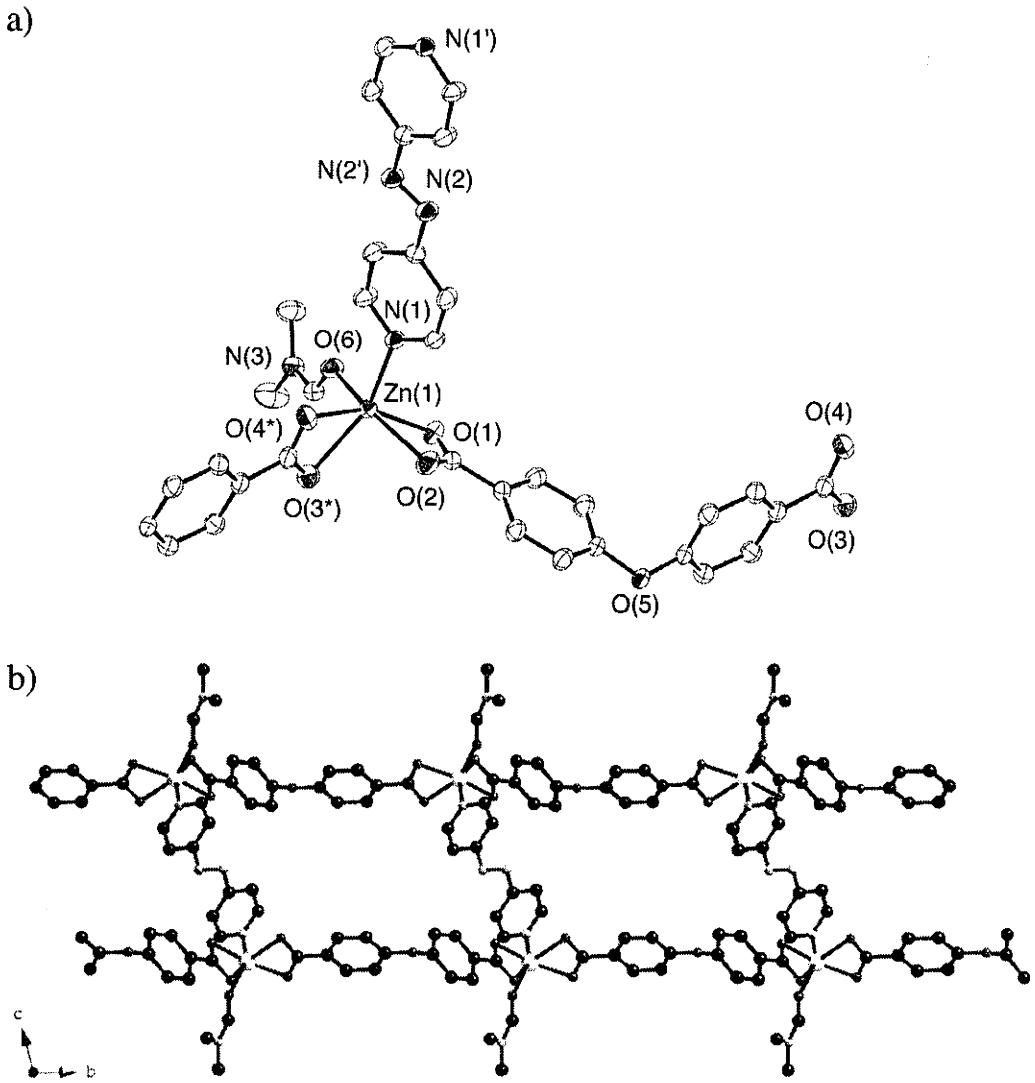

Figure 2. View of Compound **3**. ORTEP diagram around the zinc center at 30% probability (a) and the ladder type one-dimensional structure (b).

Despite having large cavities, the ladder frameworks stack along the direction of the (*a*+*c*) vector without interpenetration. Although the oba ligands of the chain are located between the two cavities of different adjacent chains, the cavities are large enough to form crevices, which are connected to create one-dimensional channels directed along the (*a*+*c*) vector. The channels are filled with three free dmf molecules per one zinc atom.

The single crystals of Compound **4** were grown using a similar procedure to that used to prepare Compound **3**. An ORTEP view around the zinc centers is shown in Figure 2a. The selected bond distances and angles are listed in Table 2. The dinuclear zinc centers in Compound **4** are supported by the four carboxylate groups of oba, in which the crystallographic inversion center is located in the central region between the two zinc atoms. The Zn···Zn distance (2.954 (2) Å) is close to that of Compound **1** (2.928 (1) Å). The pyridine nitrogen atom of the bpe group coordinates to the zinc center at the apical position, yielding a square pyramidal geometry. The Zn_2 units are connected by oba ligands to form a two-dimensional framework directed along the *bc* plane (Figure 3b). The two-dimensional framework of Zn_2-$(oba)_2$ is similar to that seen in Compound **1**. The oba ligands protrude from the layer plane, forming a significant undulating layer with a thickness of about 11 Å. Each layer contains rhombus cavities with dimensions of about 17 Å × 11 Å.

Table 2. Selected bond distances (Å) and angles (°) for Compound **4**.

Zn(1)—O(1)	2.050(5)	Zn(1)—O(2*)	2.032(6)
Zn(1)—O(3')	2.003(5)	Zn(1)—O(4'')	2.030(4)
Zn(1)—N(1)	2.019(6)		
O(1)—Zn(1)—O(2*)	159.1(2)	O(1)—Zn(1)—O(3')	88.5(2)
O(1)—Zn(1)—O(4'')	87.7(2)	O(1)—Zn(1)—N(1)	96.1(2)
O(2*)—Zn(1**)—O(3)	88.9(2)	O(2*)—Zn(1*)—O(4)	87.4(2)
O(2*)—Zn(1)—N(1)	104.7(2)	O(3')—Zn(1*)—O(4)	159.3(2)
O(3')—Zn(1)—N(1)	102.2(2)	O(4'')—Zn(1)—N(1)	98.5(2)

symmetry equivalent positions; * = 1/2-x, 1/2-y, -z, ' = x, -y, 1/2+z,
'' = 1/2-x, 1/2+y, 1/2-z

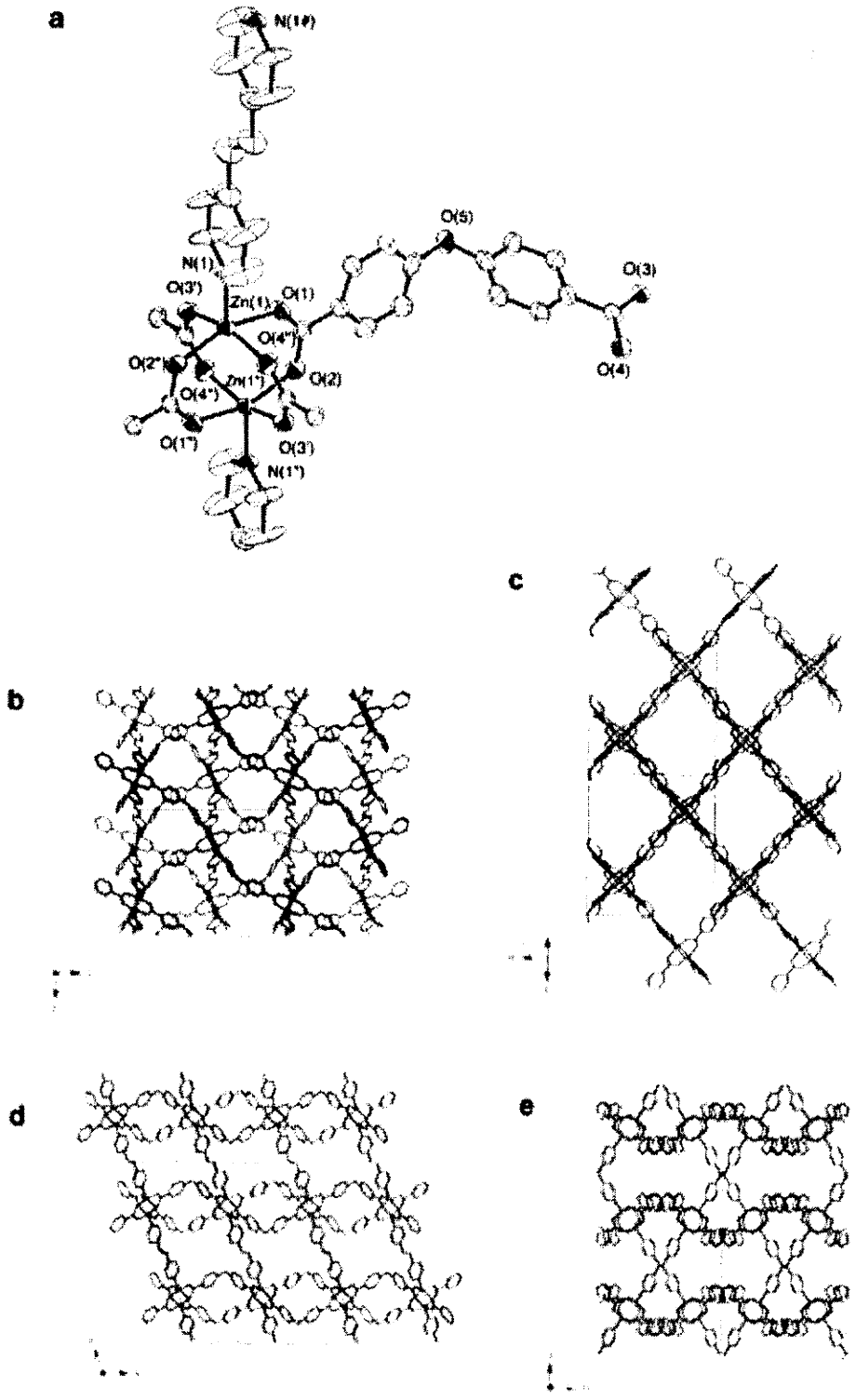

Figure 3. View of Compound **4**. ORTEP view around the dizinc center at 30% probability (a). View of the oordination framework along the *a*-axis (b), (*a*+*c*) vector (c), *b*-axis (d), and *c*-axis (e).

These layers are connected by bpe ligands that bridge two zinc centers in the adjacent layers, successfully forming a three-dimensional coordination framework constructed by two organic components. The two-dimensional layer is markedly undulated along the *b*-axis due to the distortion at the ether-oxygen atom of the oba ligands (C–O–C = 118.9(7)°), in which the Zn_2 units are located at the slant of the undulated layer, i.e., the Zn···Zn vectors are not perpendicular, but tilted by about 46° and –46°, respectively, to the *bc* plane. As a result, the Zn_2-bpe chains are not perpendicular to the *bc* plane but are aligned parallel to the (*a*+*b*) and (*a*–*b*) vectors (Figure 4).

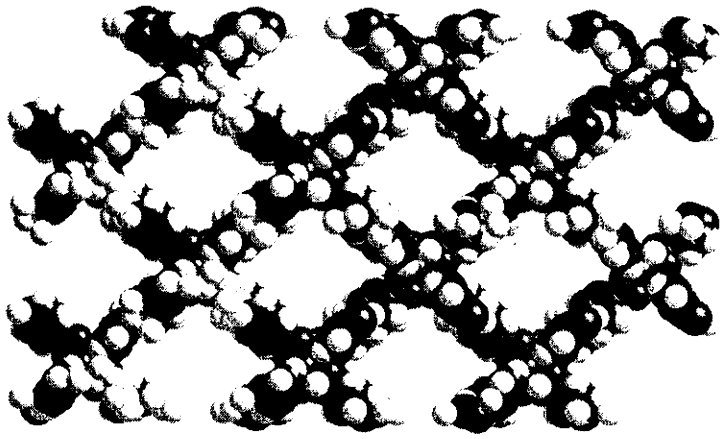

Figure 4. The aspect of the largest channel structure with van der Waals radii along the (*a*+*c*) vector.

The basic framework of Compound **3** is constructed by bridges in the two-dimensional layer in the *bc* plane composed of pillars of bpe ligands. The effectively longer Zn···Zn bond distances bridged by oba and bpe groups (about 15 Å and 13.4 Å, respectively) construct the highly porous framework. The density of the $|Zn_2(oba)_2(bpe)|$ framework is only

0.53 g cm^{-3}, reflecting the high porosity of the framework. Compound **4** has channels that are connected in three dimensions. The largest channels are directed along the (*a*+*c*) vector, as shown in Figure 3c, with an effective area of about 13 × 11 $Å^2$. In addition, three channels are observed along each axis, with areas of: 4 × 3, 6 × 4, and 11 × 3 $Å^2$ along the *a*-, *b*-, and *c*-axes, respectively. The channels are filled with two DMF molecules per dinuclear unit.

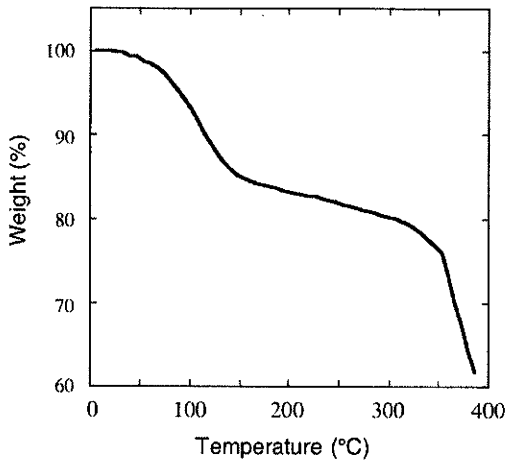

Figure 5. Thermogravimetric curve of Compound **4**.

The thermal stability of the highly porous framework of Compound **4** was estimated using thermogravimetric analysis (Figure 5). The removal of the guest DMF molecules was observed below about 200 °C (observed 18%, calcd 21%) . Any ensuing weight loss due to deformation of the resulting dry sample was not observed until 310 °C, implying a high stability of the guest-free framework of Compound **4**. A similar stability was reported in the three-dimensional coordination polymer $|M_2$(1,4-benzenedicarboxylate)L| (L = triethylenediamine, 4,4'-bipyridine) [12, 22, 23], which has similar network motifs to Compound **4**.

Characterization of the functionalities based on the highly porous framework of Compound **4** is currently in progress.

Experimental

Preparations of the compounds

The compound $[Zn_2(oba)_2(azpy)(dmf)_2]\cdot 6DMF$ (**3**) was prepared by diffusion of a DMF solution (200 mL) of H_2oba (5.2 g, 20 mmol) and azpy (6.0 g, 20 mmol) into a DMF solution (200 mL) of $Zn(CH_3COO)_2\cdot 2H_2O$ (2.2 g, 10 mmol). Red columnar crystals were formed within a period of one week, and these were collected by filtration under a nitrogen atmosphere because of the highly moisture sensitivity. Elemental analysis (%) Calcd for $C_{44}H_{62}N_6O_{24}Zn_2$ ($[Zn_2(oba)_2(azpy)(dmf)_2]\cdot 12H_2O$) : C, 44.21; H, 5.25; N, 7.06. Found: C, 44.82; H, 5.19; N, 6.69.

The compound $[Zn_2(oba)_2(bpe)]\cdot 2DMF\cdot 4H_2O$ (**4**) was prepared using a similar procedure to that used to prepare Compound **3**. A DMF solution (200 mL) of H_2oba (5.2 g, 20 mmol) and bpe (3.6 g, 20 mmol) was allowed to diffuse into a DMF solution (200 mL) of $Zn(CH_3COO)_2\cdot 2H_2O$ (2.2 g, 10 mmol). Colorless cubic crystals were formed within a period of one week, and these were collected by filtration under a nitrogen atmosphere because of the highly moisture sensitivity. One crystal of each compound was used in the single crystal X-ray analysis, and the residual crystals were used for other measurements. Elemental analysis (%) Calcd for $C_{52}H_{60}N_6O_{17}Zn_2$ ($[Zn_2(oba)_2(bpe)]\cdot 4DMF\cdot 3H_2O$) : C, 53.30; H, 5.16; N, 7.17. Found: C, 53.69; H, 4.79; N, 7.46.

Crystal structure determination

For both Compounds **3** and **4**, a suitable single crystal was sealed in a glass capillary tube along with its mother liquid. Data collection was carried out using a Rigaku CCD mercury system fitted with a monochromatic Mo Kα radiation source (λ = 0.71069 Å) at room temperature for Compound **3** and at –40 °C for Compound **4**. The X-ray data obtained is shown in Table 3. Six preliminary data frames were measured at increments of $\omega = 0.5°$ to assess the crystal quality and preliminary unit cell parameters. The intensity of the images was also measured at intervals of $\omega = 0.5°$. The intensity of the images was integrated using the Crystal Clear software package, and an empirical absorption correction was applied to the data. The structures were resolved using a direct method (SIR-92). For Compound **3**, all the nonhydrogen atoms were refined anisotropically using the full-matrix least-squares technique except for the crystalline solvent molecules, which were refined isotropically. The geometrical hydrogen atoms were placed in idealized positions, and were included, but not refined. For Compound **4**, the nonhydrogen atoms were refined anisotropically using the full-matrix least-squares technique except for the crystalline solvent DMF molecules, which were not refined, but were included. All calculations were performed using the TEXSAN crystallographic software package (Molecular Structure Corporation, USA).

Table 3. Crystal data for compounds **3**, **4**.

	3	**4**
Formula	$C_{31}\ H_{40}\ N_6\ O_9\ Zn$	$C_{46}\ H_{50}\ N_4\ O_{16}\ Zn_2$
fw	706.07	1045.68
Temperature (K)	293	233
Crystal system	Triclinic	Monoclinic
Space group	$P\bar{1}$ (# 2)	$C2/c$ (# 15)
a (Å)	9.792(6)	27.21(2)
b (Å)	14.138(8)	17.77(1)
c (Å)	14.475(8)	22.99(2)
V (Å^3)	1798(1)	10424(14)
α (°)	99.660(6)	90
β (°)	103.095(5)	110.29(1)
γ (°)	107.615(5)	90
Z	2	4
Reflcns measured	16795	34000
Unique Reflcns	9839	11896
Reflcns obs	6197 ($I > 2\sigma(I)$)	2748 ($I > 2\sigma(I)$)
No. of Variables	424	269
R	0.0821	0.0867
wR	0.0859	0.0974

Reference

[1] M. Fujita, Y. J. Kwon, S. Washizu, K. Ogura, J. Am. Chem. Soc. 116 (1994) 1151.

[2] J.-M. Lehn, Supramolecular chemistry, VCH, Weinheim, 1995.

[3] S. R. Batten, R. Robson, Angew. Chem. Int. Ed. 37 (1998) 1460.

[4] P. J. Hagrman, D. Hagrman, J. Zubieta, Angew. Chem. Int. Ed. 38 (1999) 2638.

[5] D. B. Amabilino, J. F. Stoddart, Chem. Rev. 95 (1995) 2725.

[6] D. S. Lawrence, T. Jiang, M. Levett, Chem. Rev. 95 (1995) 2229.

[7] M. Eddaoudi, D. B. Moler, H. Li, B. Chen, T. M. Reineke, M. O'Keeffe, O. M. Yaghi, Acc. Chem. Res. 34 (2001) 319.

[8] S. Kitagawa, R. Kitaura, S. Noro, Angew. Chem. Int. Ed. 43 (2004) 2334.

[9] M. Kondo, T. Okubo, A. Asami, S. Noro, T. Yoshitomi, S. Kitagawa, T. Ishii, H. Matsuzaka, K. Seki, Angew. Chem. Int. Ed. 38 (1999) 140.

[10] X.-L. Wang, C. Qin, E.-B. Wang, Y.-G. Li, Z.-M. Su, L. Xu. L. Carlucci, Angew. Chem. Int. Ed. 44 (2005) 5824.

[11] R. Kitaura, K. Fujimoto, S. Noro, M. Kondo, S. Kitagawa, Angew. Chem. Int. Ed. 41 (2002) 133.

[12] D. N. Dybtsev, H. Chun, K. Kim, Angew. Chem. Int. Ed. 43 (2004) 5033.

[13] W. Mori, K. Inoue, H. Yoshida, S. Nakayama, S. Takamizawa, M. Kishita, Chem. Lett. (1997) 1219.

[14] J. Kim, B. Chen, T. M. Reineke, H. Li, M. Eddaoudi, D. B. Moler, M. O'Keeffe, O. M. Yaghi, J. Am. Chem. Soc. 123 (2001) 8239.

[15] M. Eddaoudi, J. Kim, M. O'Keeffe, O. M. Yaghi, J. Am. Chem. Soc. 124 (2002) 376.

[16] M. Kondo, Y. Hayakawa, M. Miyazawa, A. Oyama, K. Unoura, H. Kawaguchi, T. Naito, K. Maeda, F. Uchida, Inorg. Chem. 43 (2004) 5801.

[17] H. Li, M. Eddaoudi, T. L. Groy, O. M. Yaghi, J. Am. Chem. Soc. 120 (1998) 8571.

[18] M. Kondo, M. Miyazawa, Y. Irie, R. Shinagawa, T. Horiba, A. Nakamura, T. Naito, K. Maeda, S. Utsuno, F. Uchida, Chem. Commun. (2002) 2156.

[19] M. Kondo, Y. Shimizu, M. Miyazawa, Y. Irie, A. Nakamura, T. Naito, K. Maeda, F. Uchida, T. Nakamoto, A. Inaba, Chem. Lett. (2004) 514.

[20] M. Kondo, Y. Irie, Y. Shimizu, M. Miyazawa, H. Kawaguchi, A. Nakamura, T. Naito, K. Maeda, F. Uchida, Inorg. Chem. 43 (2004) ASAP Web Release.

[21] M. L. Hu, P. Gao, S. W. Ng, Acta Cryst. C58 (2002) m323.

[22] K. Seki, Phys. Chem. Chem. Phys. 4 (2002) 1968.

[23] K. Seki, S. Takamizawa, W. Mori, Chem. Lett. (2001) 332.

Chapter 4.

Flexible Hexagonal Tube Framework of a New Nickel Complex Assembled from Intermolecular Hydrogen Bonds

Abstract

A new nickel tubular framework compound, $[Ni(ima)_2(MeOH)_2]\cdot 2MeOH$ (where ima = 4-imidazoleacetata) has been synthesized, in which the non-methanolated complex, $[Ni(ima)_2]$, selectively reacts with methanol to reconstruct the initial porous framework, which can then incorporate other guest molecules.

Introduction

The synthesis of coordination polymers with flexible channel frameworks has attracted intense attention in the development of new functional materials.[1-3] When isolated,

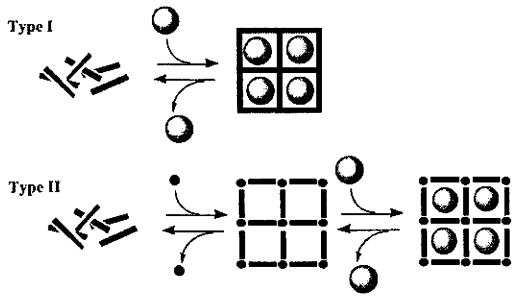

Figure 1 The two types of dynamic coordination networks. The stick assembly on the left-hand side shows the decomposed non-porous framework that is obtained by removal of guest molecules from the original porous framework (illustrated on the right-hand side). In Type I behaviour, the original porous structures are reversibly recovered by re-inclusion of the guest molecules, in which the guest molecules themselves occupy the channels. In Type II behaviour, the re-inclusion of the guest molecules reconstructs the initial porous structure that can include additional guest molecules.

coordination polymers have porous frameworks that generally include guest molecules in their channels. Although many porous coordination polymers do not retain their porous frameworks on removal of the guest molecules, they often reconstruct to form the initial porous framework by re-inclusion of the guest molecule on contact.[3] A general schematic drawing showing this reconstruction process, known as Type I behavior, is shown in Figure 1. The initial porous framework usually does not have enough space for further addition of guest molecules, as the channels are already filled with guest molecules. Therefore, reconstruction of a porous framework that has enough channel spaces for other guest molecules is attractive from the viewpoint of a new flexible network system that exhibits a porous function when triggered by a chemical stimulus. However, such dynamic network systems, illustrated as Type II behaviour in Figure 1, are still relatively unexplored.

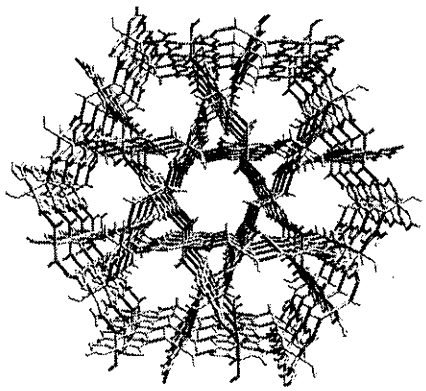

Figure 2 A view of the one-dimensional structure of **1** connected by NH··O=C intermolecular hydrogen bonds (a), and the tube-assembled structure assembled by OH··O=C intermolecular hydrogen bonds (b). The intermolecular hydrogen bonds are denoted by coloured lines.

Recently, we found that imidazole-carboxylate type chelates are useful for the synthesis of coordination frameworks connected by NH··O=C intermolecular hydrogen bonds.[4]

During further synthetic studies of assembled metal complex systems incorporating imidazole-carboxylate sets, we have prepared[Ni(ima)$_2$(MeOH)$_2$]·2MeOH (where ima = 4-imidazoleacetate) (1), and the dried, methanol-free amorphous compound [Ni(ima)$_2$] (2). Single crystal X-ray analysis shows that 1 has a porous structure constructed by hexagonal tubular frameworks that have enough space to incorporate guest molecules. We have found that 2 selectively reacts with methanol to reconstruct 1, which then can adsorb other guest molecules in the hexagonal channels. This reconstruction system is of the Type II classification shown in Figure 1.

Result and Discussion

Compound **1** was isolated as light-blue-colored columnar crystals by the diffusion of a methanol solution of the sodium salt of ima in an aqueous solution of a nickel perchlorate.† Figure 2 shows the assembled structure of **1**. This structure is isostructural to the Co analogue that was recently reported by Drozdzewski *et al.*[5] The nickel center exhibits octahedral coordination geometry surrounded by the two ima and two methanol ligands. These monomeric units are connected by two NH··O=C intermolecular hydrogen bonds (N—O = 2.758(3) Å) to yield a one-dimensional (1D) board framework along the *c*-axis (Figure 2a). The nature of the intermolecular hydrogen bonds is similar to that of [Cu(imc)$_2$]. These 1D board frameworks are further connected by OH··O=C intermolecular hydrogen bonds formed between the coordinating methanol molecules and the O=C groups of the ima (O—O = 2.623(3) Å). As a result, a unique tube-assembled framework is created (Figure 2b). The size of the crevices of the board framework, *i.e.* the 1D chain shown in Figure 2a, is < 1 Å, indicating the creation of a

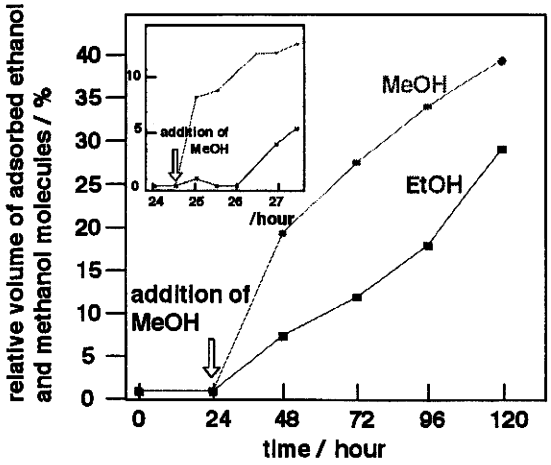

Figure 3. Plots of the relative volumes of ethanol and methanol molecules normalized against equivalent and quarter equivalent of **2**.

sterically well-isolated tube framework. Each channel, whose effective size is about 6 x 6 $Å^2$ based on the van der Waals radii, incorporates two guest methanol molecules per nickel ion. These methanol molecules, which are not located in the center of the channels but near the channel wall, form hydrogen bonds with the coordinating carboxylate oxygen atoms (O—O = 2.808(4) Å). As a result, 1 has enough space to incorporate further guest molecules in the channels. These tubular channels are connected to each other, as each board is shared between two hexagonal tube channels (Figure 2b). The resulting structure is composed of hexagonal and small trigonal columnar frameworks.

Thermogravimetric (TG) analysis shows that the included and coordinating methanol molecules are observed up until temperatures of 35 and 100 °C, respectively (see supporting information). We prepared the methanol-free dried compound $[Ni(ima)_2]$ (**2**) by heating **1** at 130 °C under reduced pressure for 2 h. Compound **2** is an amorphous solid that exhibits no X-ray powder diffraction (XRPD) peaks. We studied the reconstruction properties of **2** to form **1** on contact with guest methanol molecules by monitoring the XRPD patterns, and observed that

1 is reconstructed on exposure of **2** to methanol overnight. On the other hand, contact of **2** with water or other general organic solvents, such as ethanol, propanol, acetonitrile or acetone vapor does not yield **1** or any other crystalline solid (see supporting information). These experiments show that **2** selectively reacts with methanol to re-form **1**.

The selective reconstruction of the tubular assembled framework of **1** from the amorphous solid **2** in response to methanol exposure prompted us to study the adsorption properties against ethanol of **1** that was reconstructed by the addition of methanol to **2**. The preliminary results are shown in Figure 3, which shows plots of the relative volume of adsorbed ethanol and methanol molecules, which are normalized values against the equivalent and quarter equivalent of **2**, respectively.‡ The normalized volume of methanol adsorption reflects the rate of re-formed **1** in the reaction, and the volume of ethanol absorption reflects the molar rate of adsorbed ethanol to reconstructed **1**. Compound **2** and the equivalent volume of ethanol were immersed in *m*-xylene at 23 °C for 24 h. Even after a period of 24 h after mixing, no adsorption of ethanol was observed. After a period of 24 h, four equivalents of methanol to **2** were added to the reaction media. It was observed that the adsorption of methanol and ethanol began 1 h and 3 h, respectively, after the addition of methanol (see insert in Figure 3). The adsorption of methanol before the adsorption of ethanol could be due to an initial reaction of **2** with methanol, followed by an adsorption of ethanol in the reconstructed channels of **1**. This result demonstrates that **2** has a methanol-responsive porous function in connection with the reconstruction of the tubular framework assembly of **1**. After a period of 96 h from the addition of methanol, up to 40% of the methanol was absorbed, implying that 40% of **2** had transformed to **1** during this time. For the same period, 30% of the ethanol had been adsorbed, implying that

had adsorbed about 75% of the ethanol present. The slow reaction speed is most likely due to ıe difficulty of the methanol molecules gaining access to the center of the crystalline samples. 'urther studies on this functional system are currently in progress.

Table 1. Crystal data for compounds **1**

	1
Formula	$C_{12}H_{14}N_4NiO_8$
fw	437.08,
Temperature (K)	293
Crystal system	Triclinic
Space group	$R\bar{3}$ (# 148)
a (Å)	26.575(2)
b (Å)	26.575(2)
c (Å)	8.3321(8)
V (Å^3)	5096.1(6)
Z	9
R	0.055
*w*R	0.067

Experimental

Adsorption experiments. Compound **2** (16 mg, 0.05 mmol) was immersed in *p*-xylene (2.0 ml) containing the equivalent amount of ethanol (2.9 μl, 0.05 mmol). Four equivalents of methanol (8.0 μl, 0.20 mmol) were added to the solution after 24 h. The volume of adsorbed methanol and ethanol molecules was monitored using gas chromatography (GC). All the experiments were carried out at 23 °C.

References

1 (a) K. Kasai, M. Aoyagi and M. Fujita, *J. Am. Chem. Soc.*, 2000, **122**, 2140; (b) G. J. Halder, C. J. Kepert, B. Moubaraki, K. S. Murray and J. D. Cashion, *Science*, 2002, **298**, 1762; (c) K. Biradha and M. Fujita, *Angew. Chem. Int. Ed.*, 2002, **41**, 3392; (d) K. Biradha, Y. Hongo, and M. Fujita, *Angew. Chem. Int. Ed.*, 2002, **41**, 3395; (e)K. Uemura, S. Kitagawa, K. Fukui and K. Saito, *J. Am. Chem. Soc.*, 2004, **126**, 3817; (f) T. K. Maji, K. Uemura, H.-C. Chang, R. Matsuda, and S. Kitagawa, *Angew. Chem. Int. Ed.*, 2004, **43**, 3269; (g) O. M. Yaghi, H. Li, C. Davis, D. Richardson and T. L. Groy, *Acc. Chem. Res.*, 1998, **31**, 474.

2 (a) S. Takamizawa, E.-i. Nakata, H. Yokoyama, K. Mochizuki and W. Mori, *Angew. Chem. Int. Ed.*, 2003, **115**, 4467; (b) M. Kondo, Y. Shimizu, M. Miyazawa, Y. Irie, A. Nakamura, T. Naito, K. Maeda, F. Uchida, T. Nakamoto and A. Inaba, *Chem. Lett.*, 2004, 514.

3 (a) K. Uemura, S. Kitagawa, M. Kondo, K. Fukui, R. Kitaura, H.-C. Chang, and T. Mizutani, *Chem. Eur. J.*, 2002, **8**, 3587; (b) R. Kitaura, K. Fujimoto, S. Noro, M. Kondo and S. Kitagawa, *Angew. Chem. Int. Ed.*, 2002, **41**, 133; (c) M. P. Suh, J. W. Ko, and H. J. Choi, *J. Am. Chem. Soc.*, 2002, **124**, 10976; (d) R. Kitaura, K. Seki, G. Akiyama and S. Kitagawa, *Angew. Chem. Int. Ed.*, 2003, **42**, 428; (e) M. Kondo, Y. Irie, Y. Shimizu, M. Miyazawa, H. Kawaguchi, A. Nakamura, T. Naito, K. Maeda and F. Uchida, *Inorg. Chem.*, 2004, **43**, ASAP Web Release; (f) K. Yamada, S. Yagishita, H. Tanaka, K. Tohyama, K. Adachi, S. Kaizaki, H. Kumagai, K. Inoue, R. Kitaura, H.-C. Chang, S. Kitagawa and S. Kawata, *Chem. Eur. J.*, 2004, **10**, 1; (g) S. Kitagawa, R. Kitaura and S. Noro, *Angew. Chem.*

Int. Ed., 2004, **43**, 2334; (h) S. Kitagawa and M. Kondo, *Bull. Chem. Soc. Jpn.*, 1998, **71**, 1739.

4 M. Kondo, E. Shimizu, T. Horiba, H. Tanaka, Y. Fuwa, K. Nabari, K. Unoura, T. Naito, K. Maeda and F. Uchida, *Chem. Lett.*, 2003, 944.

5 P. Drozdzewski, B. Pawlak and T. Glowiak, *J. Mol. Struct.*, 2003, **654**, 111.

A. Altomare, G. Cascarano, C. Giacovazzo and A. Guagliardi, *J. Appl. Crystallogr.*, 1993, **26**, 343.

Chapter 5.

A New Nickel Coordination Polymer with Dynamic Channels that Mechanically Capture and Release Including Guest Molecules Responding to a Temperature Variation

Abstract

A new one-dimensional nickel(II) coordination polymer with dynamic channels was prepared and characterized. This compound has two structural phases that are switched by a temperature variation. The *closed* channel created at the low temperature mechanically captures the including guests in the channels.

Introducution

Coordination channel frameworks that change their structures in response to the physical stimuli have received intense attention because of their new functions such as molecular storage.[1] Nevertheless, such dynamic coordination frameworks have not yet been well developed. We have studied coordination polymers with sulfide in organic backbone,[2] and we have recently succeeded in synthesis of a new coordination polymer with such dynamic channels, in which the channel structures *open* and *close* above and below a critical temperature

Result and discussion

The new porous coordination polymer $[Ni(dps)_2(NO_3)_2]\cdot EtOH$ (dps = 4,4'-dipyridylsulfide) (**1**) was conveniently obtained as light-blue crystals by diffusion of dps

into the $Ni(NO_3)_2 \cdot 6H_2O$ in an ethanol solution (equation (1)). As mentioned below, **1** has two structural phases that reversibly transform, depending on the temperature. The critical temperature is in the range of −18 to 2 °C, which is easily attainable. The two structural phases observed above and below the critical temperature are designated by **1*a*** and **1*b***, respectively.

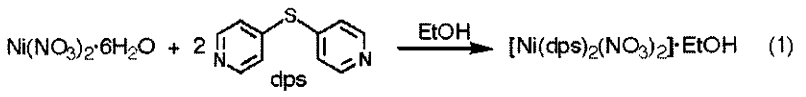

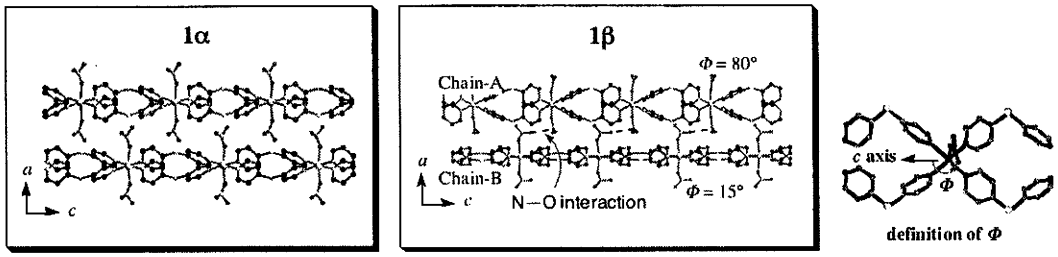

Figure 1. One-dimensional chains of **1*a*** (left) and **1*b*** (middle) are illustrated for comparison. The ethanol molecules in the channels of **1*b*** and hydrogen atoms of both compounds are omitted for clarity. The channel structures are controlled by the rotation of NO_3 anions, in which the rotation angles Φ is illustrated (right).

Figures 1 and 2 compare the arrangements of the one-dimensional chains and channel structures of **1*a*** and **1*b***.[3] **1*a***, prepared at room temperature, crystallizes in *Ccc*2. The structural determination shown in Figure 1 (left) was carried out at 23°C. The nickel center is based on a distorted octahedron with four pyridine nitrogen donors and two oxygen donors from nitrate anions. Each nickel center is bridged by two dps ligands to yield one-dimensional chains along the *c* axis. Of the four zone-dimensional chains, one-dimensional channels with a compressed octahedral shape (ca. 5 × 5 Å) are created (Figure 2). Although elemental and structural analyses at lower temperatures show that **1*a*** contains one ethanol molecule per nickel

atom, the expected electron densities were not observed in the channels due to likey the remarkable disorders at this temperature (Elemental analysis (%) calcd for $C_{22}H_{22}N_6NiO_7S_2$: 43.66; H, 3.66; N, 13.88; found: C, 43.39; H, 3.49; N, 14.11.). As a result, no atoms could be located in the channels for the X-ray refinement models.

The formation of the second structural phase was confirmed by differential scanning calorimetry (DSC) measurement and X-ray single crystal analysis. When the bulk sample of **1*a*** was cooled, followed by heating, exo- and endothermic peaks were observed with separated two peaks between –6 and –32 °C and between –19 and 2 °C, respectively. The crystal structure of the second phase, **1*b***, which forms below the critical temperature, was determined by X-ray analysis at –40 °C by using the single crystal (**1*a***) that was prepared at room temperature. The space group *C*cc2 for **1*a*** is changed to *P*nc2 for **1*b***. In contrast to **1*a***, **1*b*** contains two crystallographically independent nickel centers, which yield two types of one-dimensional chains that are made of equivalent nickel centers. The two chains are designated chain-A and chain-B as illustrated in Figure 1. The phase transformation accompanies a slide of the chain-B of about 1 Å along the *c* axis. The guest ethanol molecules, which are not structurally defined in **1*a***, are clearly observed in the channel-like cavities of **1*b***. The oxygen atom of the ethanol forms a weak hydrogen bond with an oxygen atom of a coordinating nitrate anion (O-O = 3.065(2) Å).

The slide of the chains is connected with the rotations of the nitrate anions to form electrostatic interactions[4] between nitrogen and oxygen atoms (N-O = 2.989(2) Å) in the chain-A and B. The rotation of the coordinating nitrate anions establishes the most significant effects of this transformation on the channel structures. When the angle of the NO_3 plane of

the coordinating anion to the channel direction, i.e. the *c* axis, is defined as *F*, (Figure 1) the angles of nitrate anions in **1*a*** are about 45° (and –45°). However, the *F* of nitrate anions in **1*b*** are about 80° (and –80°) and 15° (and –15°) for chain-A and chain-B, respectively. That is, the planes of the nitrate anions of chain-A are adjusted to nearly perpendicular to the channel direction. The rotations divide channel-like cavities to each cavity, in which the shape of the channel windows is changed from the "compressed hexagon" of **1a** to the "T-shape" (5 × 2 + 2 × 3 Å) by the jutting of the nitrate anions of chain-A into the channels. The structural transformation narrows the channel width from about 5 to 2 Å for the lower half of the channel window. This diminishment is sufficient to significantly change the guest capturing properties. This second phase with diminished channels is regarded as the *closed* channel phase induced by the temperature switch.

The finding of the dynamic channel framework prompted us to study the amount of ethanol molecules released from the *opened* and *closed* channels. We preliminary monitored the guest ethanol molecules released from the bulk crystalline samples of **1** as the temperature changed from –50 to 30 °C (Figure 3). When the crystalline sample was heated from –50 to 30 °C in *m*-xylene media only small concentrations of ethanol were observed, indicating that ethanol molecules are essentially not released from the cavities below –18 °C. The release of ethanol molecules was suddenly observed at –18 °C with an apparent discontinuity. Above this temperature the concentration increases with the increase in temperature, which is a typical property of physical adsorption for opened channels.

A sample cooled to –40 °C, followed by heating to room temperature, displayed similar X-ray powder diffraction (XRPD) pattern to **1*a***, and retained capturing properties for the

capture and release experiment. These results demonstrate that the *closing* and *opening* mechanism of the channels of **1** proceeds reversibly.

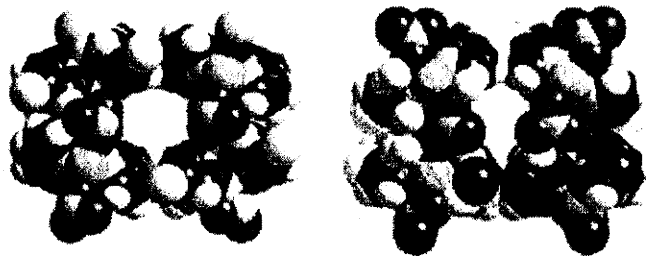

Figure 2. Channel structures with van der Waals radii of **1*a*** (left) and **1*b*** (right). This dynamic porous mechanism is unprecedented and is attractive for achieving new functionality. Further studies of the dynamic channel framework of **1** to understand the effects of the including guests on the phase transition temperature and the capturing functions against various guest molecules in gaseous and liquid states are currently undergone.

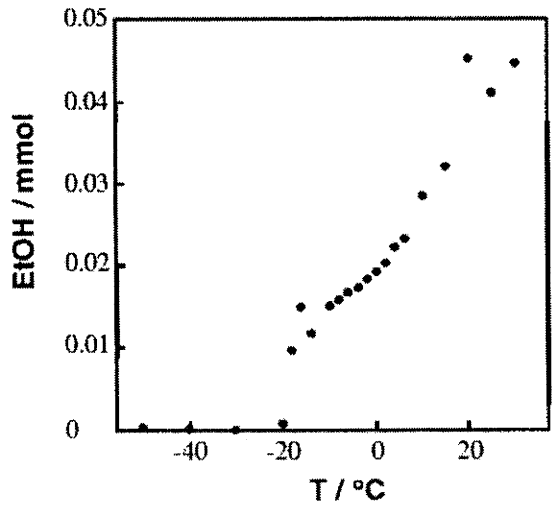

Figure 3. Plot of the amount of ethanol released from the channels of $[Ni(dps)_2(NO_3)_2]\cdot EtOH$ against temperature. The crystalline sample (100 mg, 1.7×10^{-4} mol) was cooled to -50 °C, then immersed in m-xylene (3 mL) containing a small amount of methanol (5.89 ml, 1.7×10^{-4} mol) at -50 °C. The methanol molecules in m-xylene were added to promote the release of ethanol molecules from the channels by replacement with methanol. The amount of ethanol molecules released in the m-xylene media was monitored by gas chromatography as the temperature was increased to 30 °C.

References and Notes

1 a) J. L. Atwood, L. J. Barbour, and A. Jerga, *Science* **296**, 2367 (2002). b) S. Kitagawa and M. Kondo, *Bull. Chem. Soc. Jpn.* **71**, 1739 (1998). c) P. J. Hagrman, D. Hagrman, and J. Zubieta, *Angew. Chem. Int. Ed.* 2638, **38** (1999). d) O. M. Yaghi, H. Li, C. Davis, D. Richardson, and T. L. Groy, *Acc. Chem. Res.*, **474**, 31 (1998). e) C. Janiak, *J. Chem. Soc., Dalton Trans.* **2003**, 2781. f) S. Takamizawa, E.-I. Nakata, H. Yokoyama, K. Mochizuki, and W. Mori, *Angew. Chem. Int. Ed.* 4331, **42** (2003). g) K. Uemura, S. Kitagawa, M. Kondo, K. Fukui, R. Kitaura, H.-C. Chang, and T. Mizutani, *Chem. Eur. J.* 3587, **8** (2002). h) M. Albrecht, M. Lutz, A. L. Spek, and G. van Koten, *Nature* 970, **406** (2000).

2 M. Kondo, M. Miyazawa, .Y. Irie, R. Shinagawa, T. Horiba, A. Nakamura, T. Naito, K. Maeda, S. Utsuno, and F. Uchida, *Chem. Commun.*, **2002**, 2156.

3 Crystal data for **1a**: fw = 605.27, orthorhombic, space group *Ccc*2 (no. 37), a = 13.27(1), b = 19.88(2), c = 10.100(9) Å, V = 2665(3) Å^3, Z = 4, D_c = 1.508 g cm^{-3}, m(Mo-Ka) = 0.937 mm^{-1}, T = 296 K, l = 0.07107 Å, w scans, R = 0.076, wR = 0.099 for 1641 unique reflections (R_{int} = 0.040) with $I > 2s(I)$ and 158 parameters. CCDC xxxxxxxx. Crystal data for **1b**: fw = 605.27, triclinic, space group *P*nc2 (no. 30), a = 13.1233(8), b = 19.468(1), c = 10.1241 (5) Å, V = 2586.6(2) Å^3, Z = 4, D_c = 1.554 g cm^{-3}, m(Mo-Ka) = 0.966 mm^{-1}, T = 233 K, l = 0.07107 Å, w scans, R = 0.038, wR = 0.052 for 5334 unique reflections (R_{int} = 0.027) with $I > 2s(I)$ and 344 parameters. The data collection were performed on a Rigaku-CCD Mercury system. The structures were solved by direct methods using SIR-92.[5] All non-hydrogen atoms were treated anisotoropically. The

hydrogen atoms were included but not refined.

4 R. K. R. Jetti, P. K. Thallapallly, A. Nangia, C.-K. Lam, and T. C. W. Mak, *Chem. Commun.*, **2002**, 952.

5 A. altomare, G. Cascarano, C. Giacovazzo, and A. Guagliardi, *J. Appl. Crystallogr.*, **26**, 343 (1993).

Chapter 6.

Synthesis of Redox Active Complexes with Bis-phenolate Ligands with Sulfide or Sulfoxide Units

Abstract

We report on the synthesis and crystal structures of Zn or Cu Complexes with bis-phenolate ligands with sulfide or sulfoxide Units. Although the 1-D network motif of Compound $[Zn_2(dbsf)_2(dmf)_2]$(**1**β) is the same to complex **1**, orientation of coordinationg dmf molecules and assembled patterns of the 1-D chains are different by reaction solvents. Compound $[Cu_2(tdsa)(phen)_2]\cdot 1.5EtOH$ (**2**) and [Cu(sdp)(phen)·Cu(Hsdp)(phen)(CH_3COO)] (**3**) have unique structure. And both compounds show redox activity based on sulfide or sulfoxide Unit.

Introduction

Synthesis of metal complexes with network structures has attracted intense attentions for the developments of new polymer materials, which often reveal various unique functions,[1] e.g. molecular magnetism,[2,3] molecular adsorption,[4,5] heterogeneous catalysis, non-linear optics,[6-8] and so on. For the synthesis of such functional metal complexes, utilizations of bridging ligands that functional groups are incorporated are rational strategy to obtain functional metal complexes. For example, polymer materials that sow high redox properties are important

as redox catalysts for the modification of electrodes[9-11] and biosensors.[12,13] Toward the aim, redox active coordination polymers, which have so called metal-organic-frameworks (MOFs), have successfully been constructed by using bridging ligands that ferrocene[14] and cobaltocenium units are incorporated.[15]

Chalcogen atoms have also been selected as functional groups, which are incorporated in organic bridging ligands, and yielded many MOFs. The typical ligands are summarized in Scheme 1.

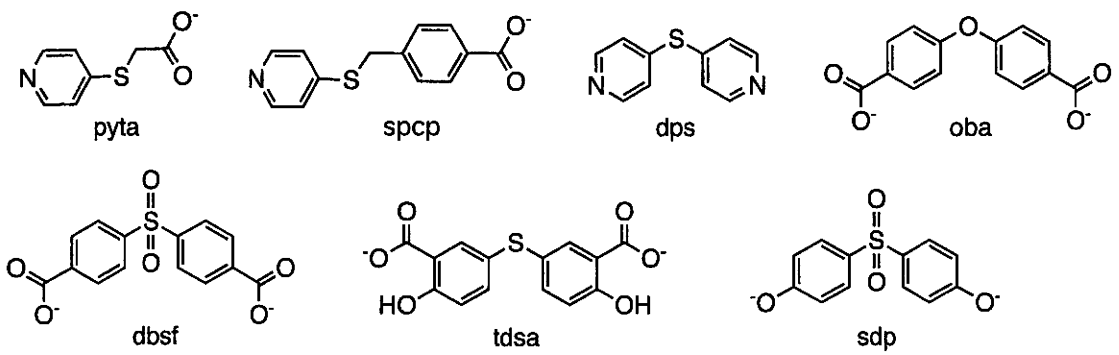

Scheme 1

For example, homo-helical frameworks were reported in [Zn(pyta)(OH)] (pyta = 4-pyridylthioacetate)[16] and [Zn(spcp)(OH)] (spcp = 4-sulfanylmethyl-4A-phenylcarboxylate pyridine).[17] The former complex [Zn(pyta)(OH)] exhibit the redox property based on the pyta moieties. On the other hand, we report the dynamic property that changes the channel structure responding to the temperature variation in $[Ni(dps)_2(NO_3)_2]EtOH$ (dps =4,4'-dipyridylsulfide).[18] This complex mechanically captures guest ethanol molecules in the close channels created in the lower temperature. Moreover, dynamic frameworks that reversibly change the infinite frameworks responding to the counter anions and present solvents were reported in

$[Ag(3,3'\text{-}Py_2S)]NO_3$ (3,3'-Py_2S = 3,3'-thiobispyridine)[19] and $[Zn_2(oba)_4(dmf)_2]$ (oba = 4,4'-oxybisbenzoate)[20] Fluorescent property was observed in $[Zn_2(dfsf)_2(dmf)_2]$ and $[Zn(dbsf)(H_2O)]$ (dbsf = 4,4'-sulfonyldibenzoate), which are 1-D network structure.[21]

As chalcogen atoms incorporating in the organic ligands, sulfur atoms (sulfide, sulfoxide, and sulfone) are more interesting compared to oxygen atoms (ether site) in the following three reasons. First, sulfide easily binds to oxygen aotms step-by-step to give sulfoxide and sulfone (Scheme 2). Second, these three groups show higher coordination ability to metal ions than ether oxygen atom, expanding the variety of network structures. This interaction is observed in $[Ag_3(dps)_2(NO_3)_3 \cdot 2H_2O]$.[22] The last, they act as redox sites, which would be useful for synthesis of redox active polymer complexes.

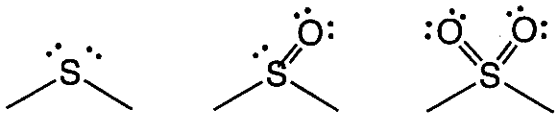

sulfide sulfoxide sulfone

Scheme 2

These ligands have often been selected to create dynamic MOFs that change the network structures in the solid state responding to external stimuli such as guest removals and reinclusions, temprature variations, and present solvents.

Recently, we have selected the three organic ligands, dbsf, 5,5'-thiodisalicylate (tdsa), and 4,4'-sulfonyldiphenolate (sdp), for constructions of new metal complexes with polymeric structure. While tdsa has a sulfur site, dbsf and sdp have a sulfone site in the skeleton. Here, we

report the synthesis, structural characterizations, and redox properties of three new metal complexes constructed by these three ligands.

Experimental Section

General. Reagents were purchased from commercial suppliers and used without further purification.

Synthesis of $[Zn(dbsf)_2(dmf)_2]\cdot 5.5DMF$ (1β). A DMF solution (100 ml) of H_2dbsf (120 mg, 0.4 mmol) was carefully diffused into a DMF solution of $Zn(CH_3COO)_2\cdot 2H_2O$ (88 mg, 0.2 mmol). One of the single crsytals obtained within a week was used for single crystal X-ray analysis. The residual crystals were used for other measurements. Elemental Analysis: Cacd for $C_{50.5}H_{68.5}N_{7.50}O_{19.50}S_2Zn_2$ ($[Zn(dbsf)_2(dmf)_2]\cdot 5.5$ DMF)

Synthesis of $[Cu(tdsa)(phen)_2]\cdot 1.5EtOH$ (2). An ethanol solution (100 ml) of $Cu(CH_3COO)_2\cdot 6H_2O$ (145 mg, 0.5 mmol) and H_2tdsa (150 mg, 0.5 mmol), and phen (90 mg, 0.5 mmol) was refluxed for 3 hours. The solution was filtered out and was stood for a few days. The crystals obtained were collected by filtration.

Synthesis of $[Cu(sdp)(phen)\cdot Cu(Hsdp)(phen)(CH_3COO)]$ (3). This complex was prepared by similar procedure for preparation of Complex **1**. An ethanol solution (100 ml) of $Cu(CH_3COO)_2\cdot 6H_2O$ (145 mg, 0.5 mmol) and H_2sdp (125 mg, 0.5 mmol), and phen (90 mg, 0.5 mmol) was refluxed for 3 hours. The solution was filtered out and was stood for a few days. The crystals obtained were collected by filtration.

Electrochemical measurements. The solid-state CV measurements were carried out by immobilization of the sample at the working electrode surface according to the

literature.[23] The glassy carbon electrode was gently rubbed over the crystalline sample (1-3 mg) for each compound in order to immobilize their compounds at the electrode surface. SCE and platinum wire were used as reference- and counter electrodes, respectively as similar to the solution-state measurements. The three electrodes were immersed in an acetonitrile solution containing tetra-*n*-buylammonium hexafluorophosphate (100 mM) as an electrite. The acetonitrile solution was degassed with nitrogen for a few minutes prior to the measurements. After each measurement, the working electrode surface was cleaned with a razor blade. Potentials versus ferrocenium/ferrocene copoule (Fc^+/Fc) were obtained by measurements with ferrocene (Fc) in the solution (about 1 mM).

X-Ray Structure Determination. For three compounds, each suitable single crystal was mounted with glue at the end of a glass fiber. Data collections were carried out on a Rigaku CCD mercury system fitted with a monochromatic Mo Kα radiation source (l = 0.71069 Å) at room temperature. The summarized data of the X-ray measurements are given in Table 1. Six preliminary data frames were measured at 0.5° increments of w, to assess the crystal quality and preliminary unit cell parameters. The intensity images were also measured at 0.5° intervals of w. The intensity images were integrated using the Crystal Clear program package, and the empirical absorption correction was applied for the data. The structures were solved by a direct method (SIR-92).

Table 1. Crystallographic Data for $[Zn_2(dbsf)_2(dmf)_2]\cdot 5.5DMF$ (**1*b***), [Cu(tdsa)]·1.5EtOH (**2**), and $[Cu(sdp)_2]$(**3**).

compoounds	**1 *b***	**2**	**3**
formula	$C_{50.5}H_{68.5}N_{7.50}O_{19.50}S_2Zn_2$	$C_{41}H_{32}CuN_4O_{7.5}0S$	$C_{56}H_{54}Cu_2N_4O_{13}S_2$
fw	1287.52	796.33	1182.27
lattice	triclinic	triclinic	monoclinic
a, Å	12.12 (1)	10.41 (2)	10.72(5)
b, Å	13.108 (8)	12.93 (3)	19.18(4)
c, Å	*20.67 (2)*	15.32 (2)	13.04(3)
a, °	70.83 (4)	66.9 (2)	90
b, °	70.80 (5)	72.3 (2)	97.59(1)
g, °	78.28 (5)	87.7 (2)	90
V, Å^3	3007 (3)	1801.2 (6)	2658.1(1)
space group	*P*1- (No. 2)	*P*1- (No. 2)	$P2_1$ (No. 4)
Z	2	2	2
r(calcd) g cm^{-3}	1.422	1.468	1.477
m(MoK*a*), mm^{-1}	0.944	0.724	0.948
radiation (*l*, Å)	0.71069	0.71069	0.71069
temp, °C	25	25	25
reflns collected	13204	16268	16729
unique relfns	4865	7828	7217
Param refined,	434	496	613
R	0.0979	0.061	0.0840
wR	0.0837		0.1239
GOF	1.190	0.834	1.302

[a] $R_1 = S||Fo| - |Fc||/S|Fo|$.

[b] $wR_2 = \{S[w(Fo^2-Fc^2)^2]/ S[w(Fo^2)^2]\}^{1/2}$

For Complexes **2** and **3**, all non-hydrogen atoms were refined anisotropically by full-matrix least-squares technique. For Complex **1*b***, carbon atoms and other non-hydrogen atoms were refined isotropically and anisotropically, respectively, by full-matrix least-squares technique. All geometrical hydrogen atoms were placed in idealized positions, and were included but not refined. All calculations were performed using the TEXSAN crystallographic software package of Molecular Structure Corporation.

Results and Discussion

Synthesis. Complex **1*b*** was obtained by a treatment of $Zn(CH_3COO)_2$ with H_2tdsa in DMF. This synthetic procedure is well established for preparations of numerous coordination polymers. On the other hand, our initial attempts for isolations of polymer complexes by simple mixing of H_2tdsa and H_2sdp with Zn(II), Cu(II), and Co(II) sources were unsuccessful. We have successfully isolated Complexes **2** and **3** by additions of phen in the reaction mixtures of these ligands and $Cu(CH_3COO)_2$ in EtOH. The former has a network structure assembled by p-p intermolecular interactions between monomer Cu(II) complexes, while the latter is a network complex constructed by coordination bonds. The crystal structures of these three complexes have been characterized by single X-ray crystallography.

Jin et al. reported the preparation and crystal structure of $[Zn_2(dbsf)_2(dmf)_2]$ (**1**).[21] Although the 1-D network motif of Complex **1** is the same to Complex **1*β***, orientations of coordinating dmf molecules and assembled patterns of the 1-D chains are different as described in below. Complex **1** is obtained from DMF/MeOH media, while Complex **1*β*** is obtained from

only DMF media. The difference of the reaction solvents would affect the resulting crystal structures of the two complexes.

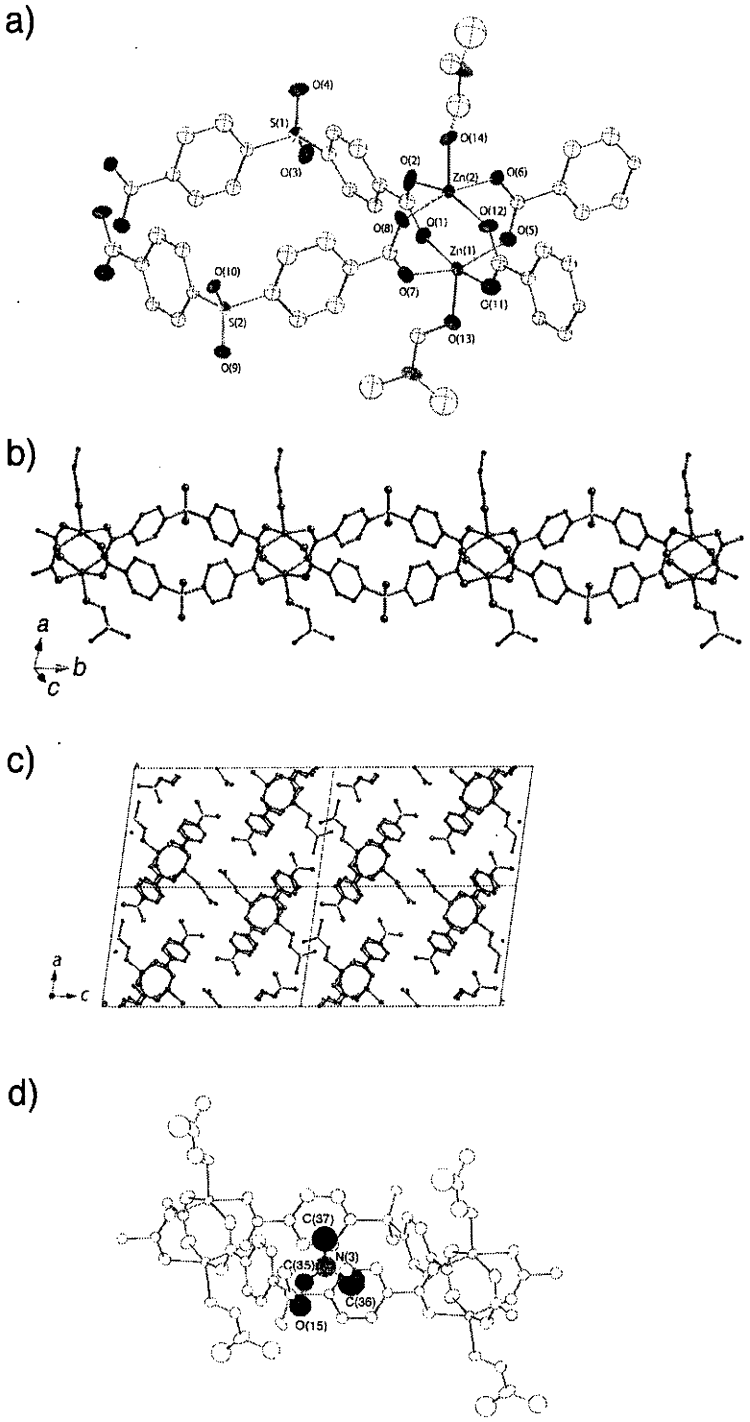

Figure 1. The views of coordination circumstance around the Zn_2 center (a) and the 1-D chain structure (b) of Complex **1**β. (b). The arrangement pattern (c) and the Zn_2-$(dbsf)_2$-Zn_2 square framework which is trapping a DMF molecule (d) are shown. The hydrogen atoms were omitted for clarity.

Numerous coordination polymers have been prepared from bis(pyridine) and bis(benzoate) type ligands. In contrast to these casese, synthetic examples constructed by bis(phenolate) type ligand are still rare.[24] On the other hand, coordination network of Complex **3** is conveniently constructed from sdp, which is a bis(phenolate) type ligand. In the case of the network structure of this complex, coordinaton of oxygen atom of sulfone to the metal ions would support the formation of the network structure.

Structure of Complex 1β. Figure 1 shows the structure of Complex **1β**. The dimeric Zn(II) units are supported by four carboxylate groups of dbsf. The Zn_2 units are connected by two dbsf ligands, yielding a 1-D chain along the *b* axis. A dmf molecule coordinates to each Zn(II) center. Although Complex **1** has been reported as a metal complex with a similar 1-D structure, Complex **1β** reveals unique difference to Complex **1** in the orientations of coordinating dmf molecules and the stacking patterns of the 1-D chains. That is, Complex **1β** is a kind of allotrope of Complex **1**.

As shown in Figures 1a and 1b, plane of coordinating dmf molecules at the one side of 1-D chain orient parallel to the chain, while that of coordinating dmf molecules at the other side orient perpendicular to the chain. This structural aspect is different to that of Complex **1**, which shows that plane of all coordinating dmf molecules orient parallel to the 1-D chain.

The stacking pattern of 1-D chains of Complexes **1β** is exhibited in Figure 1c. While 1-D chains of Complex **1** are connected by hydrogen bonds between sulfone oxygen atom and the aldehyde hydrogen atom of coordinating dmf molecule in the adjacent chains, 1-D chains of Complex **1β** do not have significant interactions to adjacent chains.

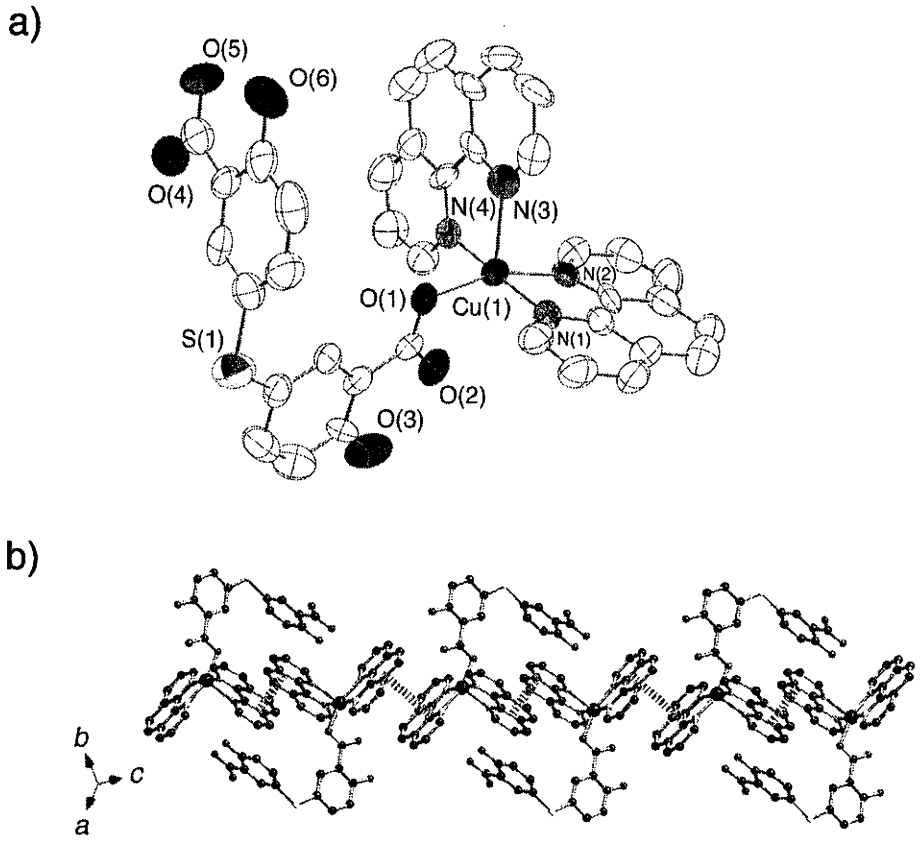

Figure 2. ORTEP view of monomeric unit of Complex **2** at 30% probability level (a) and the 1-D structure (b), in which the π-π interactions are illustrated by dashed lines. The hydrogen atoms were omitted for clarity.

While Complex **1** is a non-inclusion complex, Complex **1*β*** contains 5.5 DMF moleclues per a Zn_2 unit. Four DMF molecules are incorporated between the 1-D chains, while a DMF molecule is trapped in the Zn_2-$(dbsf)_2$–Zn_2 square in the adjacent 1-D chain (Figure 1d). Complexes **1**, **1*β***, and $[Zn_2(oba)_2(dmf)_2]$ are constructed by connections of similar Zn_2 parts by bis-benzoate ligands. in which the Zn_2 units are supported by four carboxylate groups of their ligands. Despite the similar structure of the bridging ligands, $[Zn_2(oba)_2(dmf)_2]$ gives a 2-D network, while Complexes **1** and **1*β*** give 1-D chains. This is likely the effects of C—E—C bond angles of the organic ligands. The C-S-C bond angle is generally smaller that that of

C-O-C bond angle. The C—E—C bond angles of the related complexes are summarized in Table 2. In the case of Complexes **1** and **1β** and $[Zn_2(oba)_2(dmf)_2]$, the C-S-C bond angles (105.8°) of the former complexes are smaller than that (121.6°) of C-O-C of oba ligands in the latter complexes. As bridging ligand becomes benter, the formation of the 2-D framework becomes difficult. These results are consistent with this tendency.

Table 2. Comparison of C—E—C bond angles of bridging ligands.

$[Zn_2(oba)_2(dmf)_4]]$	121.8(4)
$[Zn(oba)(H_2O)]$	122.4(9)
$[Zn(oba)_2(bpe)]2DMF$	118.9(7)
[Zn(oba)(azpy)(dmf)]2DMF	117.1(3)
Complex 1 (E = S)	105.8(2)
$[Ni(dps)_2(NO_3)_2]$ (E = S)	100.6(2)
Complex **2** (E = SO2)	103.1(7)
Complex **3** (E = SO2)	107.05

Figure 2 shows a structure of Complex **2** which is a monomeric Cu(II) complex. Four nitrogen atoms from two phen ligands and an oxygen atom from tdsa bind to the Cu(II) center, giving a square pyramidal geometry around the Cu(II) center. The apical position is occupied with a nitrogen atom of phen ligand. The Cu—N(3) bond distance (2.263 (6) Å) is significantly longer that those of other Cu—N and Cu—O bond distances (2.003 – 2.073 Å). The thioether site is bent at 106.2(4)°, which is typical for thioether bond (106.2 (4) °).

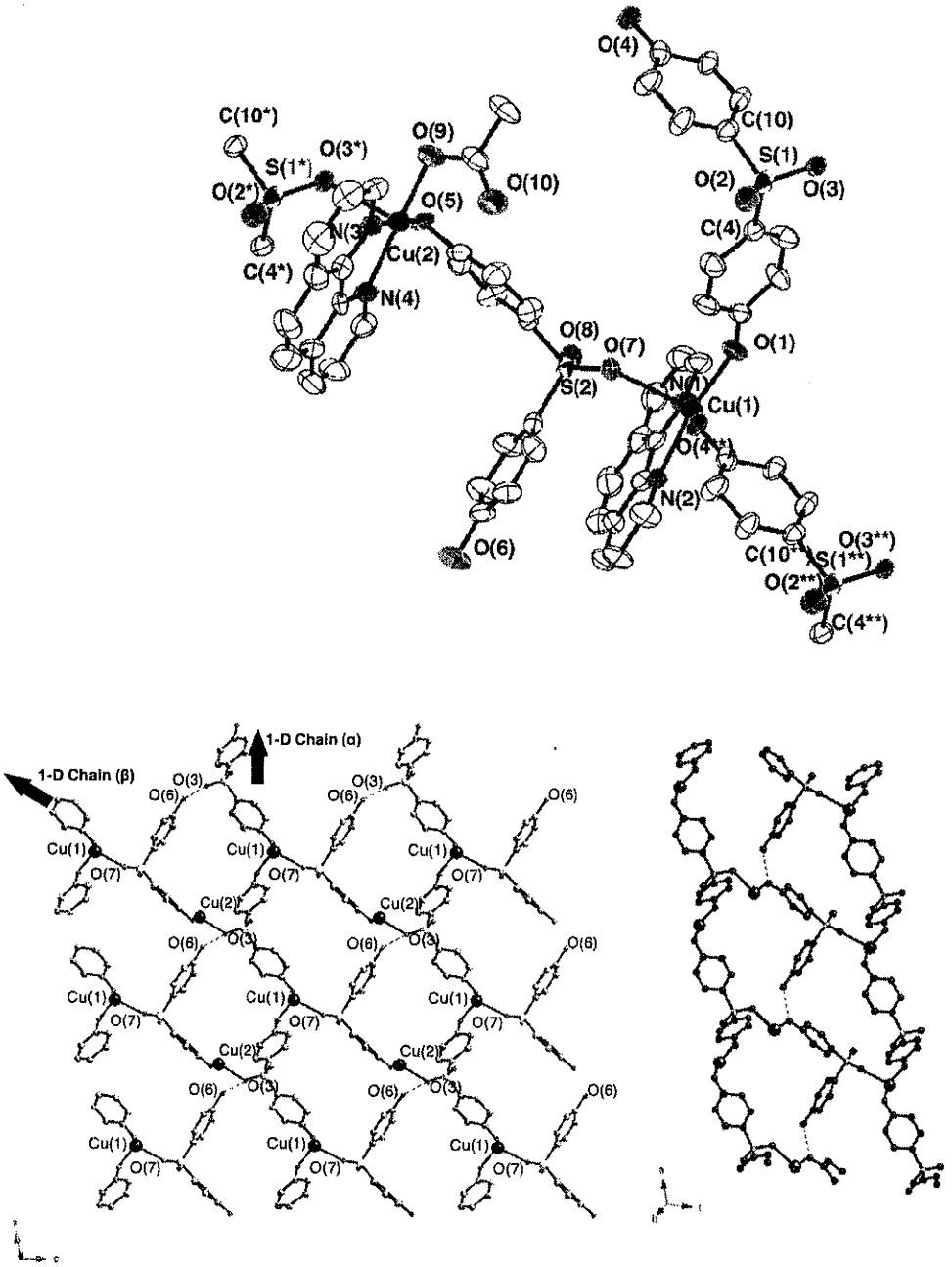

Figure 3. Structure around the coordination sites of Cu(1) and Cu(2) sites (a). Basic framework of Complex **3** is constructed by Cu(1)-sdp chains (1-D chain (α)) and {Cu(1)-(Hphs)-Cu(2)-(Hphs)} chains (1-D chain (β)) (b). The Cu(2)(Hsdp) part also forms a hydrogen bonded chains along the *a* axis (c). For structures in (b) and (c), phen and acetate ligands are omitted for clafity.

In Complex **2**, one salicylaldehyde group remains metal free. Although the positions of hydrogen atoms were not determined from Fourier Synthesis, the two carboxylate oxygen atoms would be deprotonated. The two pheol hydrogen atoms that are not deprotonated might form hydrogen bonds to the oxygen atom of the carboxylate group. As shown in Figure 2b, two units of Complex **2** gear mutually, in which the phen contact by π-π interaction with about its plane-plane distance of 3.4 Å. Each dimier contacts to the two adjacent dimers by π-π interaction with about its plane-plane distance of 3.3, yielding the 1-D chain along the (*a*+*b*-*c*) axis. This complex contains 1.5 EtOH per a Cu(II) atom. One EtOH molecule binds to O(6) atom. The other EtOH molecule was crystallographically disordered, and binds to O(6) atom at 50% of probability.

Structure of Complex **3** is exhibited in Figure 3. As shown in Figure 3a, this complex contains Cu(II) ions with quite different coordination circumstances. The Cu(1) center is based on the square pyramidal geometry with two nitrogen atoms (N(1) and N(2)) from phen, two oxygen atoms (O(1) and O(2)) from phenol oxygen atom of sdp, and a sulfone oxygen atom (O(7)) of sdp, in which the sulfone O(7) weakly coordinates to the Cu(II) center. This sulfone oxygen atom O(7) occupies the apical position. The Cu(1)—O(7) bond distance (2.395) is significantly longer than those of other Cu—N and Cu—O bonds (2.009 – 2.039 Å).

The Cu(2) center is also based on the square pyramidal geometry. The sulfone-oxygen atom (O(3)) also weakly coordinates the Cu(2) center. The two nitrogen atoms from phen, an oxygen atom from sdp, and a oxygen atom of acetate are coordinated to the Cu(2) center. The Cu(2)—O(3) bond distance is significantly longer than those of other Cu—O and Cu—N bonds (1.994 – 2.053 Å). The sulfone oxygen atom occupies the apical position.

Figures 3b illustrates the 2-D structure of Complex **3** in which phen and acetate ligands are omitted for clarity. Each Cu(1) center is bridged by sdp to yield a Cu-sdp zigzag chain along the *a* axis. The 1-D chain is designated as chain α. The *cis* coordination around the Cu(II) center and the bending at the sulfone sites of sdp give zigzag chains. As shown in Figure 3b the Cu(1) and Cu(2) centers are connected by Hphs to afford a 1-D chain along the (*a*-*c*) vector. As a result, 2-D network is constructed. The Cu(Hphs) moieties, which are nipped between the 1-D chains, are mutually connected by hydrogen bonds (O—O = 2.644 Å) between the metal-free OH of phs and coordinating O- site of phs as illustrated in Figure 3c.

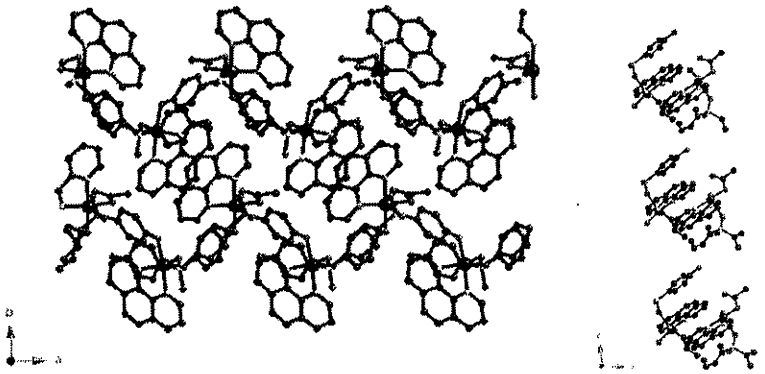

Figure 4. Overall structure of Complex 3. The 2-D layer is connected by π-π interaction yielding a 3-D network (a). The parts of π- π interactions between the layers are illustrated in (b).

Figure 4 reveals the 3-D structure of Complex **3**. The phen ligand binds to each Cu(II) site of this complex. The phen ligands stick out from the layer. These phen ligands stack with the phen ligands in the adjacent layers. The plane-plane distance between the phen ligands is about 3.5 Å. This interactions afford 3-D network.

Redox properties. Since the tdsa, dbsf, and sdp ligands are redox active ligands, the network materials obtained from these ligands would demonstrate redox activities. We have

characterized the redox properties of these complexes by measurements of cyclic voltmomgram (CV) in the solid state. Figure 5 shows the CV charts of these three complexes and the corresponding ligands, which were measured for comparisons. H_2tdsa reveals the irreversible oxidation at 2020 mV. This oxidation wave is also observed at around 2010 mV for Complex **2**. As shown in Figure 5c, irreversible reduction peak of H_2dbsf is observed at 1675 mV. The corresponding peak is clearly observed at 1750 mV for Complex **3**.

Network materials with redox activities have been prepared by using redox active ligands. Ferroecen has widely selected for the preparations. For example, Mochida et al. have shown that the crystal structures and redox properties of network materials incorporating ferrocene moieties. We have also demonstrated that the network materials obtained from cobaltoceniumdicarboxylate provide redox active network material. On the other hand, Noro et al. have shown that the loosely incorporated azopyridine in the network structure give redox property. We have also focused on the bridging ligands with thioether to create the redox active network materials. In addition to these redox active groups, we have shown that the sulfone is also redox active functional groups in this work.

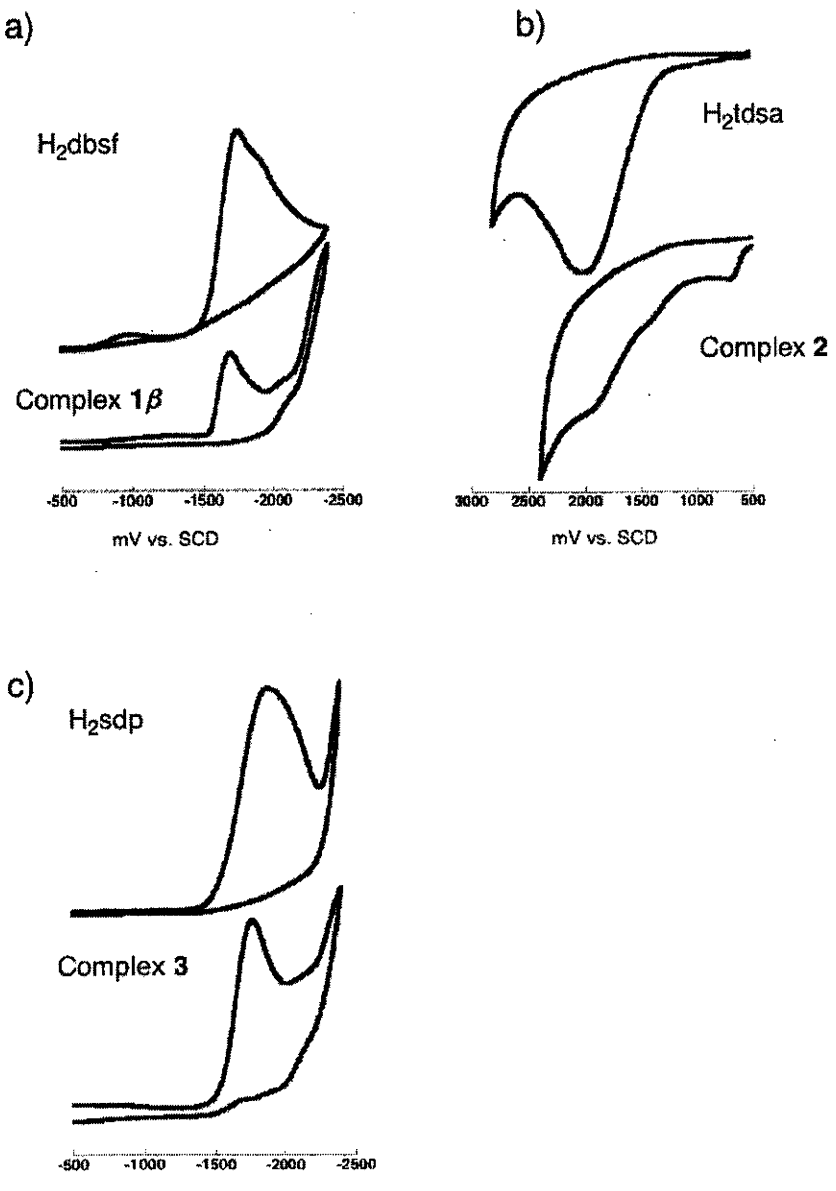

Figure 5. Cyclic voltammograms of Complex **1** and H_2tdsa (a), Complex **2** and H_2dbsf (b), and Complex **3** and H_2sdp (c) in the solid state. The complexes and the ligands are shown in full lines and broaken lines respectively.

References

(1) Ockwig, N. W.; Delgado-Friedrichs, O.; O'Keeffe, M.; Yaghi, O. M. *Acc. Chem. Res.*, *38*, 176-182.

(2) Gao, E.-Q.; Yue, Y.-F.; Bai, S.-Q.; He, Z.; Yan, C.-H. *J. Am. Chem. Soc.* **2004**, *126*, 1419-1429.

(3) Zhao, X.; Liang, D.; Liu, S.; Sun, C.; Cao, R.; Gao, C.; Ren, Y.; Su, Z. *Inorg. Chem.* **2008**, *47*, 7133-7138.

(4) Dincaˇ, M.; Yu, A. F.; Long, J. R. *J. Am. Chem. Soc.* **2006**, *128*, 8904-8913.

(5) Lin, X.; Blake, A. J.; Wilson, C.; Sun, X. Z.; Champness, N. R.; George, M. W.; Hubberstey, P.; Mokaya, R.; Schröder, M. *J. Am. Chem. Soc.* **2006**, *128*, 10745-10753.

(6) Janiak, C. *Dalton Trans.* **2003**, 2781-2804.

(7) Kesanli, B.; Lin, W. *Coord. Chem. Rev.* **2003**, *246*, 305-326.

(8) Lin, W.; Wang, Z.; Ma, L. *J. Am. Chem. Soc.* **1999**, *121*, 11249-11250

(9) Bordwell, F. G.; Cooper, G. D.; Morita, H. *J. Am. Chem. Soc.* **1957**, *79*, 376.

(10) Smith, T. W.; Kunder, J. E.; Wychick, D. *J. Polym. Sci.* **1976**, *14*, 2433.

(11) Flanagan, J. B.; Margel, S.; Bard, A. J.; Anson, F. C. *J. Am. Chem. Soc.* **1978**, *100*, 4248.

(12) Degani, Y.; Heller, A. *J. Phys. Chem.* **1987**, *91*, 1285.

(13) Hill, H. A. U.; Page, D. J.; Walton, N. J. *J. Electroanal. Chem.* **1987**, *217*, 141.

(14) Horikoshi, R.; Mochida, T.; Moriyama, H. *Inorg. Chem.* **2002**, *47*, 3017-3024.

(15) Kondo, M.; Hayakawa, Y.; Miyazawa, M.; Oyama, A.; Unoura, K.; Kawaguchi, H.; Naito, T.; Maeda, K.; Uchida, F. *Inorg. Chem.* **2004**, *43*, 5801-5803.

(16) Kondo, M.; Miyazawa, M.; Irie, Y.; Shinagawa, R.; Horiba, T.; Nakamura, A.; Naito, T.; Maeda, K.; Utsuno, S.; Uchida, F. *Chem. Commun.* **2002**, 2156-2157.

(17) Han, L.; Hong, M.; Wang, R.; Luo, J.; Lin, Z.; Yuan, D. *Chem. Commun.* **2003**, 2560-2581.

(18) Kondo, M.; Shimizu, Y.; Miyazawa, M.; Irie, Y.; Nakamura, A.; Naito, T.; Maeda, K.; Uchida, F.; Nakamoto, T.; Inaba, A. *Chem. Lett.* **2004**, 514-515.

(19) Jung, O.-S.; Kim, Y. J.; Lee, Y.-A.; Chae, H. K.; Jang, H. G.; HOng, J. *Inorg. Chem.* **2001**, *40*, 2105-2110.

(20) Kondo, M.; Irie, Y.; Shimizu, Y.; Miyazawa, M.; Kawaguchi, H.; Nakamura, A.; Naito, T.; Maeda, K.; Uchida, F. *Inorg. Chem.* **2004**, *43*, ASAP Web Release.

(21) Zhuang, W.-J.; Jin, L.-P. *Appl. Organometal. Chem.* **2007**, *21*, 76-82.

(22) Jung, O.-S.; Park, S. H.; Park, C. H.; Park, J. K. *Chem. Lett.* **1999**, 923-924.

(23) Schröder, U.; Scholz, F. *Inorg. Chem.* **2000**, *39*, 1006-1015.

(24) Jia, J.; Blake, A. J.; Champness, N. R.; Hubberstey, P.; Wilson, C.; Schröder, M. *Inorg. Chem.* **2008**, *DOI: 10.1021/ic800422g*, Release on Web.

Chapter 7

A New Redox-Active Coordination Polymer with Cobalticinium Dicarboxylate

Abstract:

A new two-dimensional coordination polymer with cobalticinium 1,1'-dicarboxylate (ccdc) incorporated in the framework has been prepared, the ccdc functioning as unique monoanionic dicarboxylate ligands. The compound shows a high redox activity based on the ccdc units.

Introduciton

Coordination polymers with metallocene units in the framework have attracted intense interest for the development of new redox-active crystalline solids,[1-9] with ferrocene moieties having mainly been utilized as the redox-active units. While ferrocene shows a redox potential due to the Fe(III)/Fe(II) couple at about 0.6 V ($E_{1/2}$) vs. SCE, cobaltocene shows the Co(III)/Co(II) couple at a quite different potential, about –0.9 V.[10,11] This large difference in the M(III)/M(II) redox potentials results in the different oxidation states for these units that are generally observed at ambient conditions.[12,13] That is, Fe(II) and Co(III) states are the most convenient oxidation states for ferrocene and cobaltocene units, respectively.[11,12] Although coordination polymers with cobaltocene or cobalticinium units in the framework are promising compounds that show different redox properties compared with those for ferrocene units, the coordination polymers constructed by cobaltocene units are still unexplored. We have selected

cobalticinium 1,1'-dicarboxylate (ccdc; Scheme 1) as bridging ligands toward the synthesis of new redox-active crystalline materials. Here we report the synthesis and structural characterization of a new coordination polymer $[Cu(ccdc)_2]\cdot 2MeOH$ (**1**). An additional unique feature of this type of network is the creation of coordination frameworks with mixed metal ions, studies of which are still rare.

The Hccdc was prepared by oxidation of 1,1'-dimethylcobalticinium with potassium permanganate according to the literature.[12] **1** was isolated as green plate crystals by diffusion of a methanol solution of $Cu(CH_3COO)_2\cdot H_2O$ into a DMF solution of Hccdc.† The crystal structure was determined by X-ray diffraction studies.‡ **1** crystallizes in the asymmetric space group $P4_3$. Figure 1 shows the coordination center and crystal structure of **1**, which contains two crystallographically independent ccdc units and a copper ion. Four oxygen atoms of the carboxylate groups from ccdc bind to the copper(II) center to form a distorted square planar geometry. Each ccdc connects two copper(II) centers to yield a two-dimensional structure with small square cavities (about 4 × 4 Å) in the *ab* plane (Figure 1b).

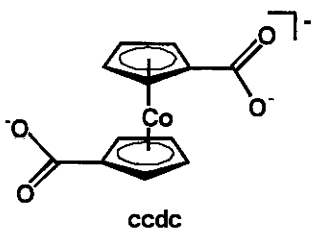

ccdc

Scheme 1

Because the two cp rings of ccdc can rotate, this ligand acts as a flexible connector between the metal ions. When the torsion angle Φ of the two carboxylate groups of ccdc is

defined as in Scheme 2, the steric configurations are generally classified following six patterns;[9] Synperiplanar (0°), Synclinal-Staggered (36°) Synclinal-Eclipsed (72°), Anticlinal-Staggered (108°), Anticlinal-Eclipsed (144°), and Antiperiplanar (180°). For **1**, the Φ are about 162° and 157° for the two crystallographically independent ccdc units with Co(1) and Co(2) centers, respectively. That is, both carboxylate groups of ccdc show a conformation between Anticlinal-Eclipsed and Antiperiplanar. As a result, ccdc connects between two copper(II) centers with slightly bent angles from 180°.

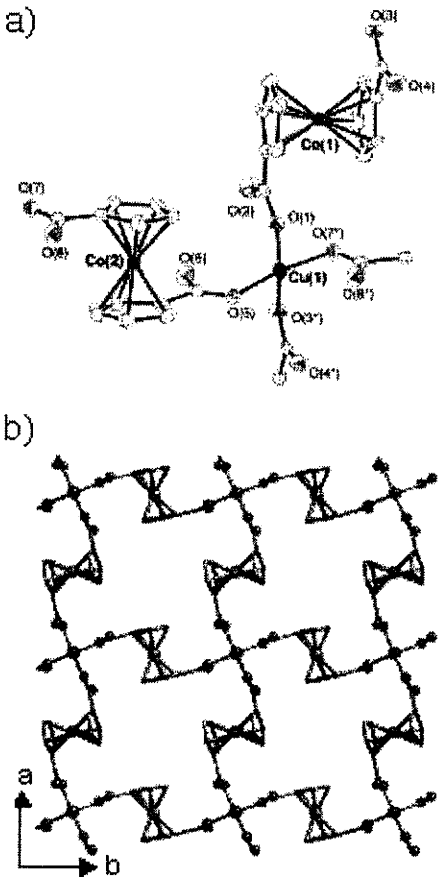

Figure 1. ORTEP view of the crystal structure of **1** (a) (30% probability level) and views of the two-dimensional structure (b). Hydrogen atoms and methanol molecules are omitted for clarity.

Scheme 2

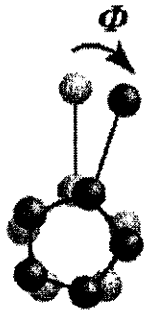

These layers stack along the *c* axis in an ABCD pattern with 90° rotation (Figure 2), in which the four crystallographic screw axes run through the cavities of the layer. Each square cavity is capped from above and below by ccdc units in the adjacent layers, creating closed cavities with dimensions of about 4 × 4 × 6 $Å^3$ in the crystal. These spaces are connected by small crevices with sizes of about 2 × 1 Å. As a result, each cavity, which traps methanol molecules, is well isolated from the outside. To the best of our knowledge, this is the first example of a coordination polymer with cobalticinium units incorporated in the framework.

The unique feature of the ccdc ligand compared with other general organic dicarboxylate ligands is the difference of the charge.[14] When the neutral coordination frameworks are constructed by combination of dianionic dicarboxylate ligands with divalent metal ions, the ratio of the ligand to metal ions of the frameworks would be 1:1 because of the charge balance. That is, when the dicarboxylate groups simply connect metal ions as bis-monodentate ligands, a one-dimensional framework is formed. For example, 1,1'-ferrocenedicarboxylate (fcdc) produces a 1:1 salt with Cd(II) ion to yield

[Cd(fcdc)(dmf)$_2$(H_2O)] with a zigzag chain framework.[3] In contrast to this case, **1** creates a two-dimensional framework, which consists of a 2:1 ratio of ccdc with Cu(II) ion. This result implies that the charge of the dicarboxylate ligands, which is controlled by the oxidation states of the metal ions of the metallocene units, has a large effect on the network motifs of the coordination frameworks.

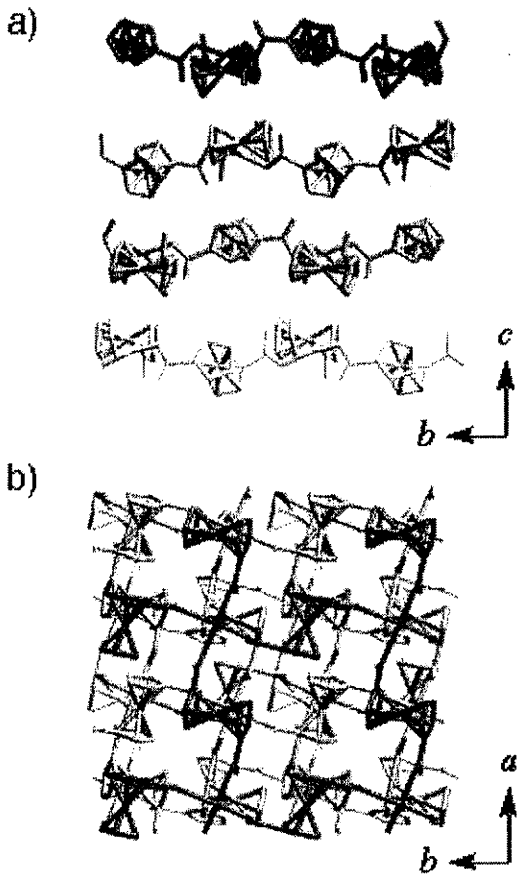

Figure 2. The stacking aspect showing the ABCD pattern along the *a* axis (a) and the *c* axis (b), in which each layer is shown by different colors. Hydrogen atoms and methanol molecules are omitted for clarity.

The construction of this new coordination network with cobalticinium units prompted us to study the redox properties of **1**. When the cyclic voltammogram (CV) of ccdc was measured in a DMF solution, the quasi-reversible couple was observed at –1414 mV (vs. Fc^+/Fc), as shown in Figure 3a, in which the ccdc was prepared in a DMF solution by addition of an equivalent amount of triethylamine. The corresponding redox couple based on the cobalticinium units of **1** was observed at –1709 mV by a solid state CV measurement (Figure 3b). The solid state CV measurement of ccdc was difficult in water or general organic media because of the high solubility of either ccdc or the reducing product. The negative shift (295 mV) of the redox potential of **1** from that of ccdc is not negligible since our previous studies indicate that the solid state redox potentials of the sulfide or ferrocene groups incorporated in the coordination frameworks reveal similar redox potentials compared to the free ligands in the solution.[8,15] The negative shift of the redox potential of **1** is in contrast to the expectation of an electron-withdrawing effect by the dipositive charge of the copper(II) ions. This could be the result of donation from the dπ orbital of Cu(II) ions to the anti-bonding orbital of ccdc. A similar negative shift is observed in Ag complexes with ferrocene units.[16]

Redox-active bridging ligands do not always produce redox-active coordination networks. For example, redox-active azopyridines do not show any redox properties when they are incorporated in coordination networks.[17] On the other hand, the network system described above shows a high redox property based on the ccdc units, demonstrating that the metallocene is an effective bridging unit for creation of new redox-active network materials. The redox potential is remarkably more negative than that of the coordination compounds with

ferrocene units. Further characterization and synthetic studies with ccdc are currently underway.

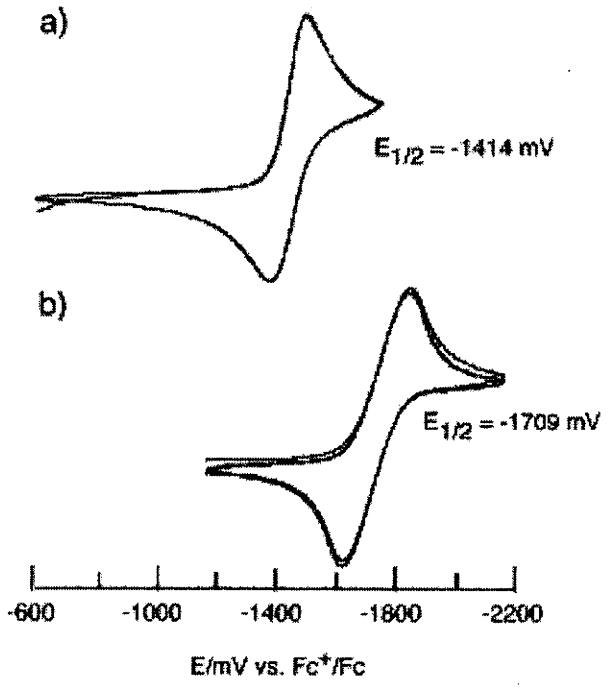

Figure 3. Cyclic voltammograms of ccdc in DMF solution in the presence of triethylamine (a) and **1** in the solid state (b).

References and Notes

† One of the single crystals were used for single X-ray analysis. The residual sample was used for other measurements. Anal. Calc. For $C_{26}H_{30}Co_2CuO_{13}$ (**1**·$3H_2O$): C,42.67; H, 4.13; Found. C, 43.15; H, 3.58%.

‡ Crystallographic data for **1**: $C_{26}H_{24}Co_2CuO_{10}$, M = 677.9, tetragonal, space group $P4_3$ (no. 78), $a = b$ = 10.550(5), c = 23.15(1) Å, V = 2576(2) $Å^3$, Z = 4, D_c = 1.747 g cm^{-3}, μ(Mo-Kα) =

2.419 mm^{-1}, $F(000)$ = 1372, T = 293 K, λ = 0.7107 Å, ω scan, R = 0.058, wR = 0.060 for 3057 unique reflections (R_{int} = 0.047) with $I > 2\sigma(I)$ and 332 parameters. The data collection was performed on a Rigaku CCD Mercury system. The structure was solved by direct methods using SIR-92.[18] All non-hydrogen atoms were treated anisotropically. Hydrogen atoms were included but not refined.

(1) Prokopuk, N.; Shriver, D. F. *Inorg. Chem.* **1997**, *36*, 5609-5613.

(2) Oh, M.; Carpenter, G. B.; Sweigart, D. A. *Acc. Chem. Res.* **2004**, *37*, 1-11.

(3) Dong, G.; Hong, M.; Chun-ying, D.; Feng, L.; M., Q.-j. *J. Chem. Soc., Dalton Trans.* **2002**, 2593-2594.

(4) Okamura, T.; Sakauye, K.; Ueyama, N.; Nakamura, A. *Inorg. Chem.* **1998**, *37*, 6731-6736.

(5) Horikoshi, R.; Mochida, T.; Moriyama, H. *Inorg. Chem.* **2002**, *47*, 3017-3024.

(6) Braga, D.; Cojazzi, G.; Abati, A.; Maini, L.; Polito, M.; Scaccianoce, L.; Grepioni, F. *J. Chem. Soc., Dalton Trans.* **2000**, 3969-3975.

(7) Yao, H.; Sabat, M.; Grimes, R. N.; de Biani, F. F.; Zanello, P. *Angew. Chem. Int. Ed.* **2003**, *42*, 1002-1005.

(8) Kondo, M.; Shinagawa, R.; Miyazawa, M.; Kabir, M. K.; Irie, Y.; Horiba, T.; Naito, T.; Maeda, K.; Utsuno, S.; Uchida, F. *J. Chem. Soc., Dalton Trans.* **2003**, 515-516.

(9) Dong, G.; Yu-ting, L.; Chun-ying, D.; Hong, M.; Quing-jin, M. *Inorg. Chem.* **2003**, *42*, 2519-2530.

(10) Baik, M.-H.; Friesner, R. A. *J. Phys. Chem. A* **2002**, *106*, 7402-7412.

(11) Gloaguen, B.; Astruc, D. *J. Am. Chem. Soc.* **1990**, *112*, 4607-4609.

(12) Sheats, J. E.; Rausch, M. D. *J. Org. Chem.* **1970**, *35*, 3245-3248.

(13) Braga, D.; Cojazzi, G.; Maini, L.; Polito, M.; Grepioni, F. *Chem. Commun.* **1999**, 1949-1950.

(14) Braga, D.; Maini, L.; Polito, M.; Rossini, M.; Grepioni, F. *Chem.—Eur. J.* **2000**, *6*, 4227-4235

(15) Kondo, M.; Miyazawa, M.; Irie, Y.; Shinagawa, R.; Horiba, T.; Nakamura, A.; Naito, T.; Maeda, K.; Utsuno, S.; Uchida, F. *Chem. Commun.* **2002**, 2156-2157.

(16) Lindner, E.; Zong, R.; Eichele, K.; Weisser, U.; Ströbele, M. *Eur, J. Inorg. Chem.* **2003**, 705-712.

(17) Noro, S.; Kondo, M.; Ishii, T.; Kitagawa, S.; Matsuzaka, H. *J. Chem. Soc., Dalton Trans.* **1999**, 1569-1574.

(18) Altomare, A.; Cascarano, G.; Giacovazzo, C.; Guagliardi, A. *J. Appl. Crystallogr.* **1993**, *26*, 343.

Chapter 8.

Summary and Conclusion

I have developed new coordination polymers, which change their structures responding to chemical solvents such as H_2O, MeOH, DMF. These complexes show unique structural transformations between two structures by contact with the solvents. Particularly, I have clarified the creations and lost of channel structures by the structural changes. I have shown that addition of MeOH induces the molecular adsorption of larger adsorption of EtOH molecules, in which EtOH molecules are not adsorbed before of addition of MeOH. These functions are useful for inducing the molecular adsorption by chemical stimuli.

In addition to the above system, dynamic channels that change the channel structures responding to temperature variation are also unprecedented new function. The observation of mecanical capture of the guest molecules in the closed channels and release from the open channel is novel observation, and would be applicable as various functional materials.

I have also studied syntheses and characterizations of new coordination polymers with flexible redox active ligands. The high redox activities clarified by electrochemical measurements reveal the utilities of as new electrode, biosensors, electron sources or acceptors.

List of publication (査読付き)

1. M. Kondo, Y. Shimizu, M. Miyazawa, Y. Irie, A. Nakamura, T. Naito,K. Maeda, F. Uchida, T. Nakamoto, A. Inaba "A New Nickel Coordination Polymer with Dynamic Channels that Mechanically Capture and Release Including Guest Molecules Responding to a Temperature Variation"
Chem. Lett. **2004**, 514-515.

2. M. Kondo, Y. Hayakawa, M. Miyazawa, A. Oyama, K. Unoura, H. Kawaguchi, T. Naito, K. Maeda, F. Uchida "A New Redox-Active Coordination Polymer with Cobalticinium Dicarboxylate"
Inorg. Chem. **2004**, *43*, 5801-5803.

3. M. Kondo, Y. Irie, Y. Shimizu, M. Miyazawa, H. Kawaguchi, A. Nakamura, T. Naito, K. Maeda, F. Uchida "Dynamic Coordination Polymers with 4,4'-oxybis(benzoate). Reversible Transformations of Nano- and Non-porous Coordination Frameworks Responding to Present Solvents."
Inorg. Chem. **2004**, *43*, 6139-6141.

4. M. Kondo, T. Iwase, Y. Fuwa, T. Horiba, M. Miyazawa, T. Naito, K. Maeda, S. Yasue, F. Uchida "Flexible Hexagonal Tube Framework of a New Nickel Complex Assembled from Intermolecular Hydrogen Bonds"
Chem. Lett. **2005** *34*, 410-411.

5. M. Kondo, Y. Irie, M. Miyazawa, H. Kawaguchi, S. Yasue, K. Maeda, F. Uchida "Synthesis and structural determination of new multidimensional coordination polymers with 4,4'-oxybis(benzoate) building ligands: Construction of coordination polymers with heteroorganic bridges"
J. Organomet. Chem. **2007**, *692*, 136-141.

6. 宮澤　誠、近藤　満　「外部刺激に応答して可逆的に構造を変化させる高次元型金属錯体結晶」触媒 2008、Vol. 50 No. 4, pp. 308-312.

7. M. Kondo, M. Amano, T. Iwase, M. Miyazawa, S. Yasue, K. Maeda, F. Uchida "Interlayered Host Created by Assemblies of Monomeric Nickel Complex with Imidazole-4-acetate Chelate Ligands"
Chem. Lett. **2008**, *37*, 992-993.

8. M. Miyazawa, Y. Irie, K. Kashimoto, N. Nishina, M. Kondo, S. Yasue, K. Maeda, F. Uchida "Syntheses, characterizations, and redox behaviors of new self-assembled metal complexes with bridging ligands incorporating chalcogen sites"
Inorg. Chem. Comm. . **2009**, 336-339.

Other papers（査読付き）

1. M. Kondo, M. Miyazawa, Y. Irie, R. Shinagawa, T. Horiba, A. Nakamura, T. Naito, K. Maeda, S. Utsuno, F. Uchida, "A new Zn(II) coordination polymer with 4-pyridylthioacetate: assemblies of homo-chiral helices with sulfide sites"
Chem. Commun. **2002**, 2156-2157

2. M. Kondo, R. Shinagawa, M. Miyazawa, Md. K. Kabir, Y. Irie, T. Horiba, T. Naito, K. Maeda, S. Utsuno, F. Uchida, "A New Nano-scale Ferrocene Assembled Molecule Supported by a Supercubane Framework"
J. Chem. Soc., Dalton Trans. **2003**, 515-516.

3. E. Shimizu, M. Kondo, Y. Fuwa, R. P. Sarker, M. Miyazawa, M. Ueno, T. Naito, K. Maeda, F. Uchida "Synthesis and Synthesis and Crystal Structures of Metal Complexes with 4,5-Imidazole-dicarboxylate Chelates: Self-assembled Structures via NH···O=C Intermolecular Hydrogen Bonds"
Inorg. Chem. Commun. **2004**, *7*, 1191-1194.

4. M. Kondo, Y. Shibuya, K. Nabari, M. Miyazawa, S. Yasue, K. Maeda, F. Uchida "New [2 × 2] Cyclic Framework that Induces Distortions from Square Planar to Tetrahedral around the Copper(II) Centers"
Inorg. Chem. Commun. **2007**, *10*, 1311-1314.

5. M. Kondo, S. Sugahara, Y. Nakamura, M. Miyazawa, S. Yasue, K. Maeda, F. Uchida, G. Sakane, H. Kawaguchi "Self-assembling Construction of Novel Nanoscale Heptacobalt Complex with a S-Shaped Folding"
Cryst. Eng. Commun. **2008**, 10, 1516-1516.

査読無し

1. 平川　剛、宮澤　誠、仁科直子、近藤　満「高選択的に過塩素酸イオンを除去できる高分子錯体の開発」ケミカルエンジニアリング（特集　注目される新技術の実用化）2008年9月号661-664(依頼執筆)